Recent studies within the Subtracted Second RPA

Danilo Gambacurta
gambacurta@lns.infn.it
INFN-LNS Catania

MOdeling Nuclear STructure and REactions

CO EX 7

7th International Conference on
Collective Motion in Nuclei under Extreme Conditions
Catania 11-16 June 2023

Outline

Theoretical background:

- From RPA to Second RPA (SRPA): motivations and first applications
- SRPA issues: improving on the SRPA, the Subtracted SRPA (SSRPA)

Applications

- Low-lying dipole modes:
  - Pygmy Dipole Resonance (PDR)
  - Beyond mean field effects on the EoS (J,L)
- Low-lying monopole excitations: soft modes (versus PDR)
- Most recent applications: Gamow Teller Excitations and β decay

Outline

Theoretical background:

- From RPA to Second RPA (SRPA): motivations and first applications
  D. G. et al.: PRC 81, 054312 (2010) and PRC 84, 064602 (2011)
- SRPA issues: improving on the SRPA, the Subtracted SRPA (SSRPA)
  D. G. et al.: PRC 92, 034303 (2015); Phys. Rev. Lett. 125 (2020)

Applications

- Low-lying dipole modes:
  - Pygmy Dipole Resonance (PDR)
  - Beyond mean field effects on the EoS (J,L)
- Low-lying monopole excitations: soft modes (versus PDR)
- Most recent applications: Gamow Teller Excitations and β decay

The Random Phase Approximation (RPA)

- The RPA is a widely used approach to describe collective excitations
- It provides global properties: centroid energies and total strength
- Very successful especially within the Energy Density Functional framework (interactions á la Skyrme or Gogny, covariant versions)
- Interaction parameters fitted at mean field level (Binding energies, charge radii, Nuclear Matter properties, ...)

However, extensions of the RPA are required for:

- Spreading Width
- Fine Structure and Strength Fragmentation
- Low Lying excitations in closed shell nuclei
- Double exctiations and Anharmonicities, ...

The Second RPA (SRPA): more general excitation operators are introduced

Phonon Operators: RPA vs SRPA

Random Phase Approximation (RPA)

$$Q_\nu^\dagger = \underbrace{\sum_{ph} X_{ph}^{(\nu)} \underbrace{a_p^\dagger a_h}_{\text{1p-1h}} - \sum_{ph} Y_{ph}^{(\nu)} \underbrace{a_h^\dagger a_p}_{\text{1h-1p}}}$$

Only Landau Damping, Centroid Energy and Total Strength of GRs

Second Random Phase Approximation (SRPA)

$$Q_\nu^\dagger = \sum_{ph} (X_{ph}^{(\nu)} a_p^\dagger a_h - Y_{ph}^{(\nu)} a_h^\dagger a_p)$$

$$+ \underbrace{\sum_{p_1<p_2, h_1<h_2} (X_{p_1 h_1 p_2 h_2}^{(\nu)} \underbrace{a_{p_1}^\dagger a_{h_1} a_{p_2}^\dagger a_{h_2}}_{\text{2p-2h}} - Y_{p_1 h_1 p_2 h_2}^{(\nu)} \underbrace{a_{h_1}^\dagger a_{p_1} a_{h_2}^\dagger a_{p_2}}_{\text{2h-2p}})}$$

Spreading Width, Fragmentation, Double GRs and Anharmonicites, Low-Lying States

RPA Phonon Operators

$$Q_\nu^\dagger = \sum_{ph} X_{ph}^{(\nu)} a_p^\dagger a_h - \sum_{ph} Y_{ph}^{(\nu)} a_h^\dagger a_p$$

RPA Equations of Motion ($1 \mapsto$ 1p1h)

$$\begin{pmatrix} \mathcal{A}_{11} & \mathcal{B}_{11} \\ -\mathcal{B}_{11}^* & -\mathcal{A}_{11}^* \end{pmatrix} \begin{pmatrix} \mathcal{X}_1^\nu \\ \mathcal{Y}_1^\nu \end{pmatrix} = \omega_\nu \begin{pmatrix} \mathcal{X}_1^\nu \\ \mathcal{Y}_1^\nu \end{pmatrix}$$

SRPA Phonon Operators

$$Q^{\dagger}_{\nu} = \sum_{ph} (X^{(\nu)}_{ph} a^{\dagger}_{p} a_{h} - Y^{(\nu)}_{ph} a^{\dagger}_{h} a_{p})$$

$$+ \sum_{p_1<p_2, h_1<h_2} (X^{(\nu)}_{p_1 h_1 p_2 h_2} a^{\dagger}_{p_1} a_{h_1} a^{\dagger}_{p_2} a_{h_2} - Y^{(\nu)}_{p_1 h_1 p_2 h_2} a^{\dagger}_{h_1} a_{p_1} a^{\dagger}_{h_2} a_{p_2})$$

SRPA Equations of Motion (1$\mapsto$ 1p1h, 2$\mapsto$ 2p2h)

$$\begin{pmatrix} \mathcal{A}_{11} & \mathcal{A}_{12} & \mathcal{B}_{11} & \mathcal{B}_{12} \\ \mathcal{A}_{21} & \mathcal{A}_{22} & \mathcal{B}_{21} & \mathcal{B}_{22} \\ -\mathcal{B}^{*}_{11} & -\mathcal{B}^{*}_{12} & -\mathcal{A}^{*}_{11} & -\mathcal{A}^{*}_{12} \\ -\mathcal{B}^{*}_{21} & -\mathcal{B}^{*}_{22} & -\mathcal{A}^{*}_{21} & -\mathcal{A}^{*}_{22} \end{pmatrix} \begin{pmatrix} \mathcal{X}^{\nu}_{1} \\ \mathcal{X}^{\nu}_{2} \\ \mathcal{Y}^{\nu}_{1} \\ \mathcal{Y}^{\nu}_{2} \end{pmatrix} = \omega_{\nu} \begin{pmatrix} \mathcal{X}^{\nu}_{1} \\ \mathcal{X}^{\nu}_{2} \\ \mathcal{Y}^{\nu}_{1} \\ \mathcal{Y}^{\nu}_{2} \end{pmatrix}$$

Computationally very demanding

- First applications (in the 80s' and '90s) were done resorting to strong approximations and/or small model spaces
- See, for example, S. Drodz, S. Nishizaki, J. Speth and J. Wambach *et al.*, Physics Reports 197, 1 (1990)
- Full large scale SRPA calculations have been performed:
  P. Papakonstantinou and R. Roth, PLB 671, 356 (2009);
  D.G et al. PRC 81, 054312 (2010)
- Model spaces large enough to preserve EWSRs
- No approximation in the evaluation of the matrix elements

Computationally very demanding

- First applications (in the 80s' and '90s) were done resorting to strong approximations and/or small model spaces
- See, for example, S. Drodz, S. Nishizaki, J. Speth and J. Wambach *et al.*, Physics Reports 197, 1 (1990)
- Full large scale SRPA calculations have been performed:
  P. Papakonstantinou and R. Roth, PLB 671, 356 (2009);
  D.G et al. PRC 81, 054312 (2010)
- Model spaces large enough to preserve EWSRs
- No approximation in the evaluation of the matrix elements
- Full large scale calculations show some SRPA's issues

SRPA anomalies and the Subtraction procedure

Large scale SRPA calculations have shown that:

- The SRPA strength distribution is sistematically shifted towards lower energies compared to the RPA one
- This shift is very strong ($\simeq$ 3-4 MeV), RPA description often spoiled

Origins and Causes:

1. Quasi Boson Approximation and stability problems in SRPA
2. Use of effective interactions in beyond-mean field methods

The Subtraction procedure (I. Tselyaev Phys. Rev. C 75, 024306 (2007))

- Designed for beyond RPA approaches
- It restores the Thouless theorem, e.g. instabilities are removed
- Static ($\omega = 0$) limit of the SRPA imposed to be equal to the RPA one

From SRPA to an Energy dependent RPA-like problem

- The SRPA problem as an energy-dependent RPA problem

$$A_{1,1'} \mapsto \tilde{A}_{1,1'}(\omega) = A^{RPA}_{1,1'} + \sum_{2,2'} A_{1,2}(\omega + i\eta - A_{2,2'})^{-1} A_{2',1'} = A^{RPA}_{1,1'} + A^{Cor}_{1,1'}(\omega)$$

The Subtraction procedure

From SRPA to an Energy dependent RPA-like problem

- The SRPA problem as an energy-dependent RPA problem

$$A_{1,1'} \mapsto \tilde{A}_{1,1'}(\omega) = A^{RPA}_{1,1'} + \sum_{2,2'} A_{1,2}(\omega + i\eta - A_{2,2'})^{-1} A_{2',1'} = A^{RPA}_{1,1'} + A^{Cor}_{1,1'}(\omega)$$

The Subtraction procedure is SRPA (SSRPA)

- Subtraction of the zero–frequency limit of the SRPA correction

$$A^{Cor}_{1,1'} \mapsto \tilde{A}^{Cor}_{1,1'}(\omega) = A_{1,1'}(\omega) - A_{1,1'}(\omega = 0) \Rightarrow$$

$$\tilde{A}_{1,1'}(\omega = 0) = A^{RPA}_{1,1'}$$

$$\Rightarrow \Pi^{SSRPA}(\omega = 0) = \Pi^{RPA}$$

The Subtraction procedure

From SRPA to an Energy dependent RPA-like problem

- The SRPA problem as an energy-dependent RPA problem

$$A_{1,1'} \mapsto \tilde{A}_{1,1'}(\omega) = A^{RPA}_{1,1'} + \sum_{2,2'} A_{1,2}(\omega + i\eta - A_{2,2'})^{-1} A_{2',1'} = A^{RPA}_{1,1'} + A^{Cor}_{1,1'}(\omega)$$

The Subtraction procedure is SRPA (SSRPA)

- Subtraction of the zero–frequency limit of the SRPA correction

$$A^{Cor}_{1,1'} \mapsto \tilde{A}^{Cor}_{1,1'}(\omega) = A_{1,1'}(\omega) - A_{1,1'}(\omega = 0) \Rightarrow$$

$$\tilde{A}_{1,1'}(\omega = 0) = A^{RPA}_{1,1'}$$

$$\Rightarrow \Pi^{SSRPA}(\omega = 0) = \Pi^{RPA}$$

Numerical implementation

- Subtraction performed in diagonal approximation, e.g. $A_{2,2'} \approx \delta_{2,2'} A_{2,2}$
- Full subtraction recently performed (GT strength) [a]

[a] DG, M. Grasso, J. Engel, Physical Review Letters 125, 212501 (2020)

Quadrupole Strength Distribution in ^{16}O: RPA, SRPA and SSRPA

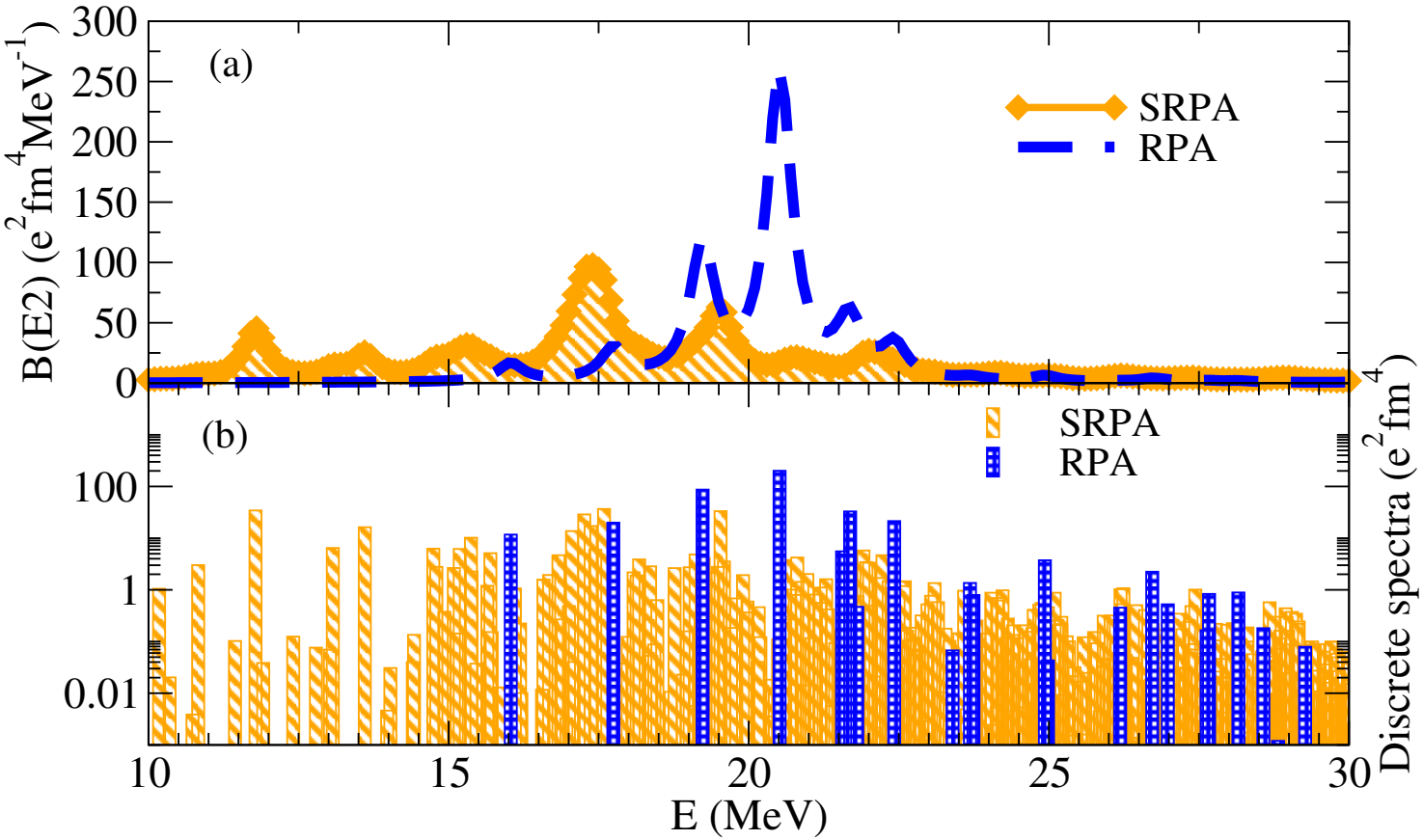

D. G., M. Grasso and J.Engel, Phys. Rev. C 92 , 034303 (2015)

Quadrupole Strength Distribution in ^{16}O: RPA, SRPA and SSRPA

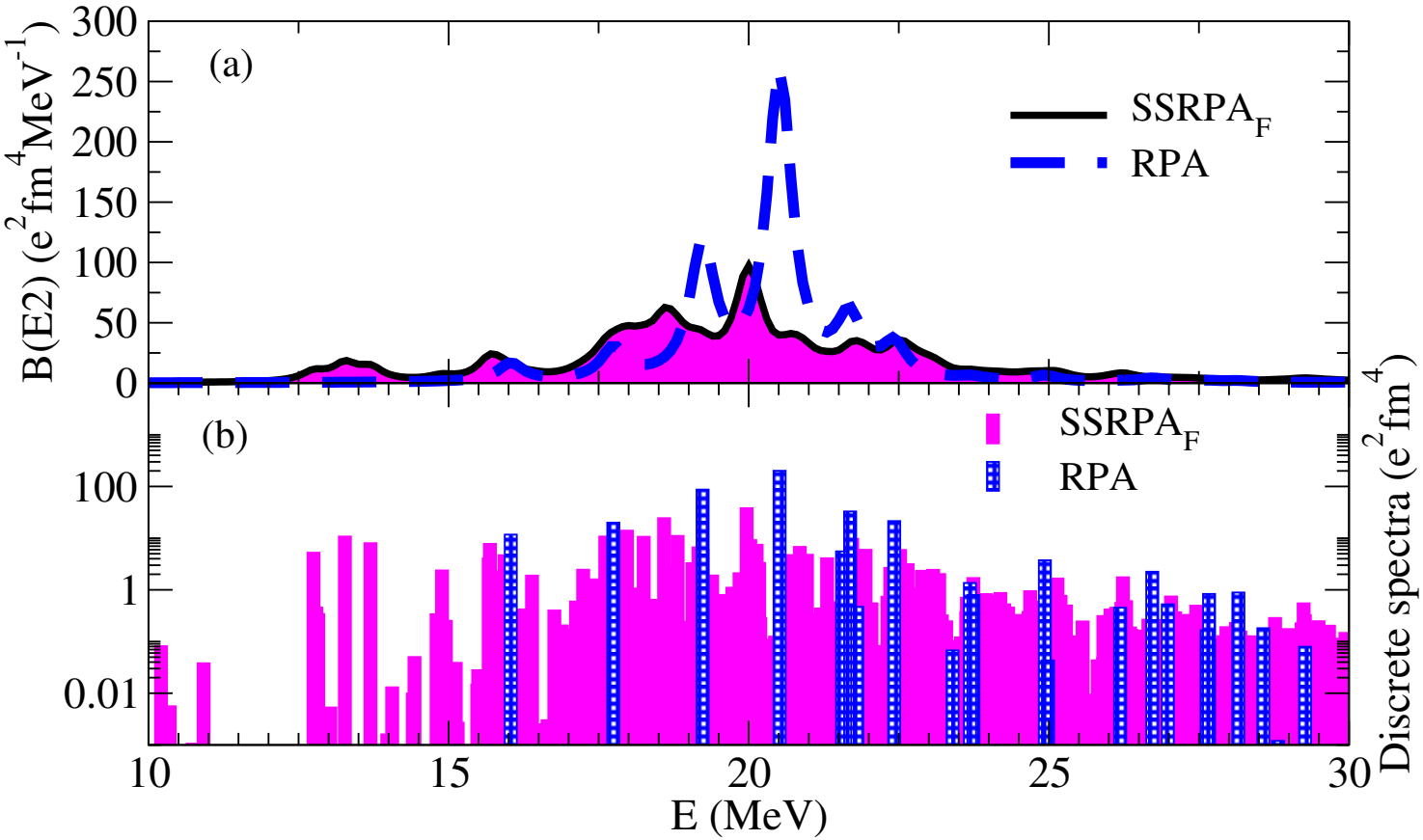

D. G., M. Grasso and J.Engel, Phys. Rev. C 92 , 034303 (2015)

Low-lying dipole response in ^{48}Ca: Motivation

- Experimental low-lying dipole (from 5 to 10 MeV) response in ^{48}Ca stronger than in ^{40}Ca
- Pygmy Dipole Resonance (PDR) type?
- Not described in relativistic and non-relativistic RPA models
- What happens in SRPA [a] and in the SSRPA [b] ?

[a] D. G. , M. Grasso, and F. Catara, Phys. Rev. C 84, 034301 (2011)
[b] D. G., M. Grasso and O. Vasseur, Physics Letters B 777 (2018) 163–168

Experimental low-lying dipole strength in ^{40},^{48}Ca. (Photon Scattering)

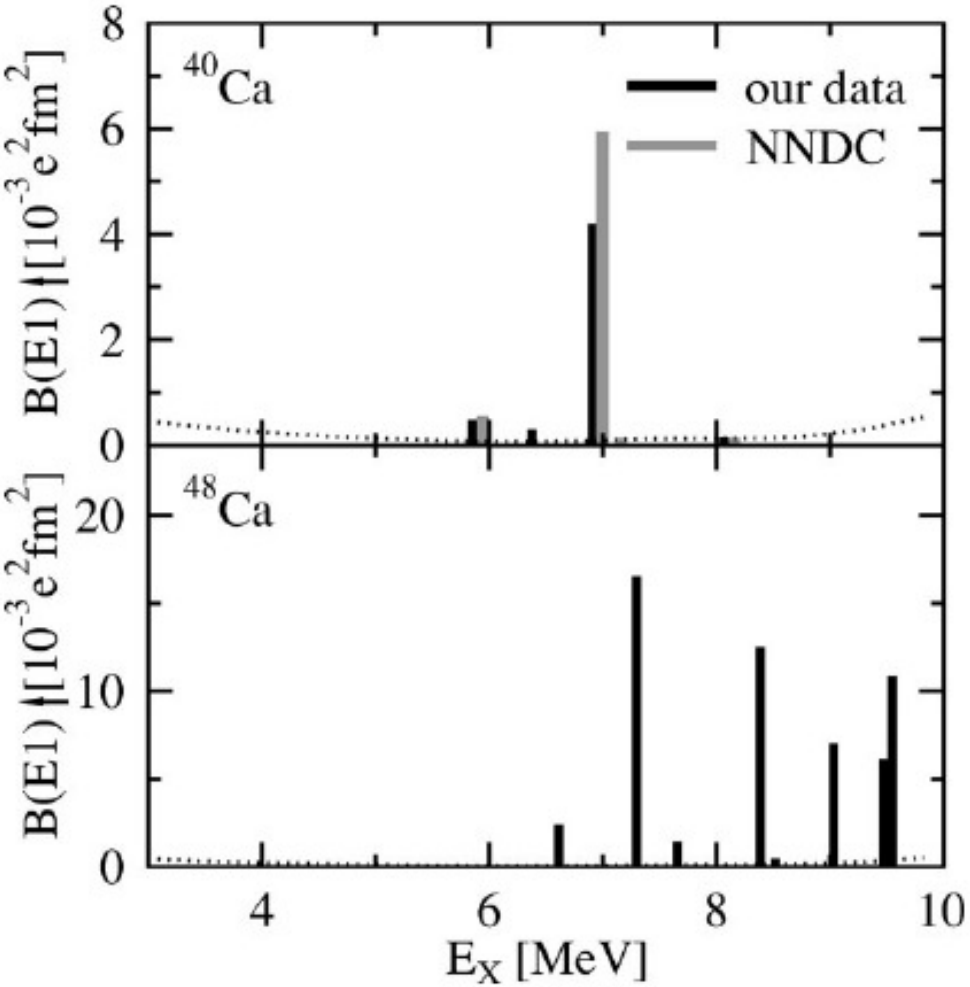

From T. Hartmann *et al.*, PRC 65, 034301, (2002)

$\sum$ B(E1)=5.1 $\pm$ 0.8 ($10^{-3}e^2fm^2$),

$\sum$ B(E1)=68.7 $\pm$ 7.5 ($10^{-3}e^2fm^2$),

RPA and SRPA Dipole Strength

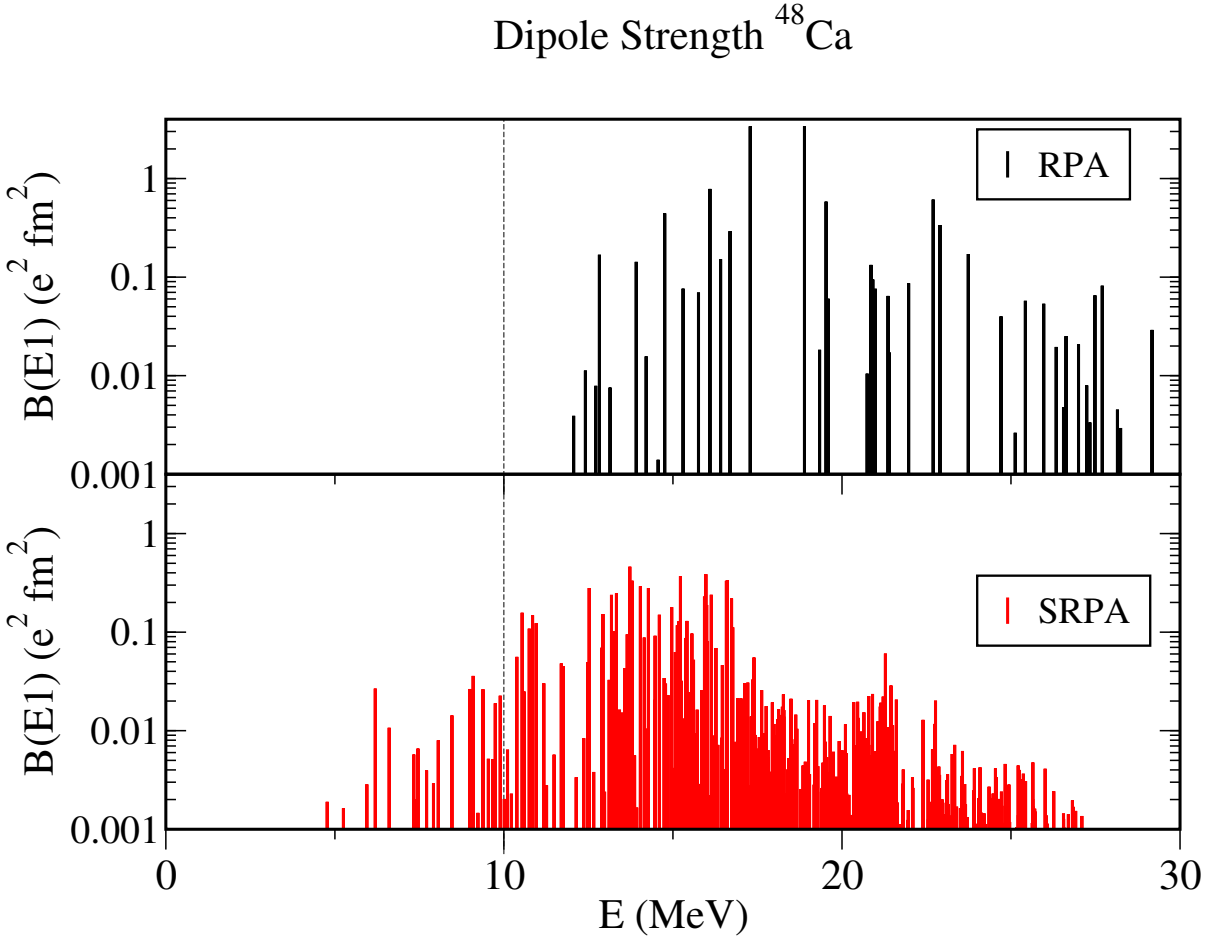

RPA and SRPA Dipole Strength

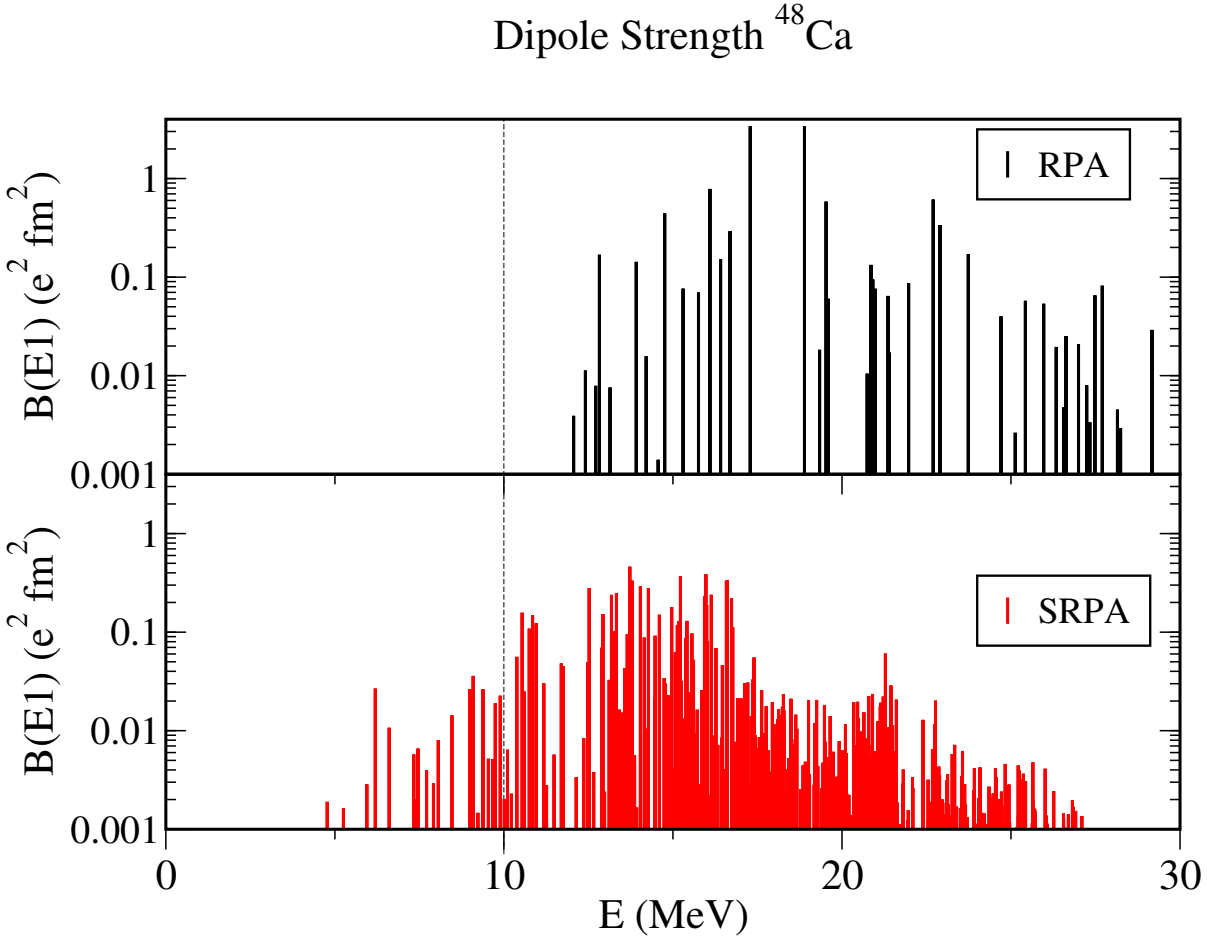

SRPA provides the strength below 10 MeV, but total strength is overestimated.

1p1h and 2p2h contents

$$\langle \nu|\nu\rangle = \sum_{ph}(\mid X^{\nu}_{ph} \mid^2 - \mid Y^{\nu}_{ph} \mid^2) + \sum_{p_1<p_2,h_1<h_2} (\mid X^{\nu}_{p_1h_1p_2h_2} \mid^2 - \mid Y^{\nu}_{p_1h_1p_2h_2} \mid^2)$$

$$= \quad N_1 \quad + \quad N_2 \quad = 1$$

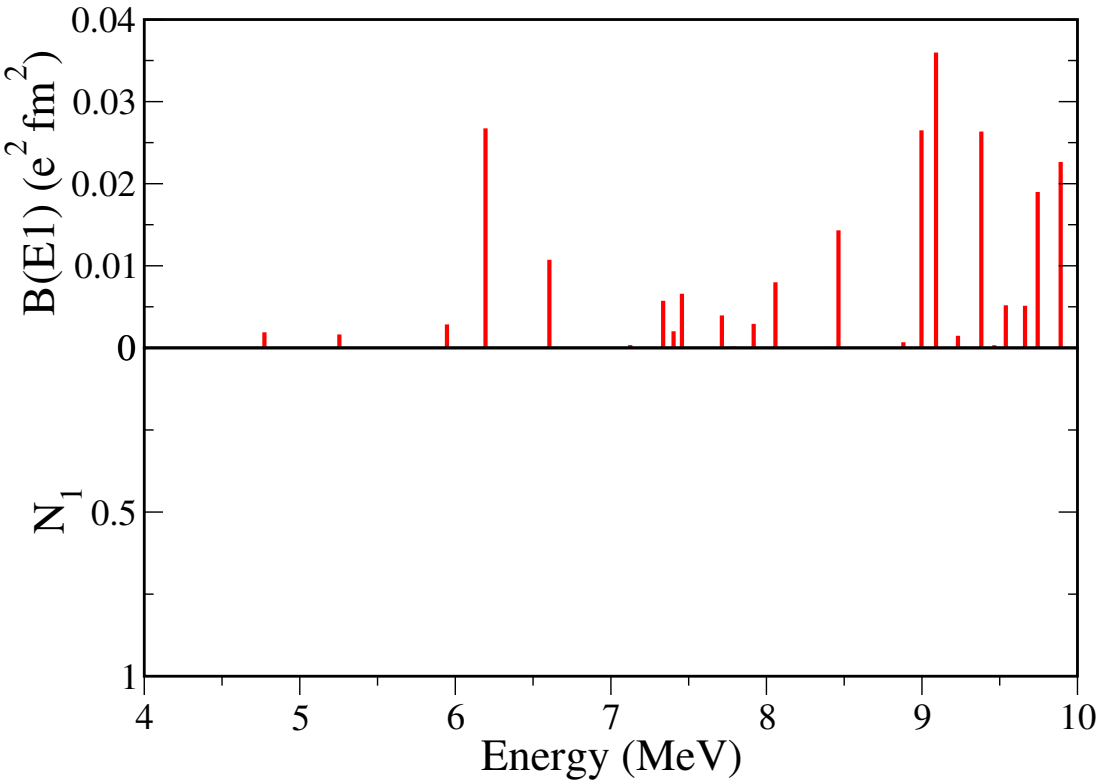

1p1h and 2p2h contents

$$\langle \nu|\nu\rangle = \sum_{ph}(\mid X^{\nu}_{ph} \mid^2 - \mid Y^{\nu}_{ph} \mid^2) + \sum_{p_1<p_2,h_1<h_2} (\mid X^{\nu}_{p_1h_1p_2h_2} \mid^2 - \mid Y^{\nu}_{p_1h_1p_2h_2} \mid^2)$$

$$= \quad N_1 \quad + \quad N_2 \quad = 1$$

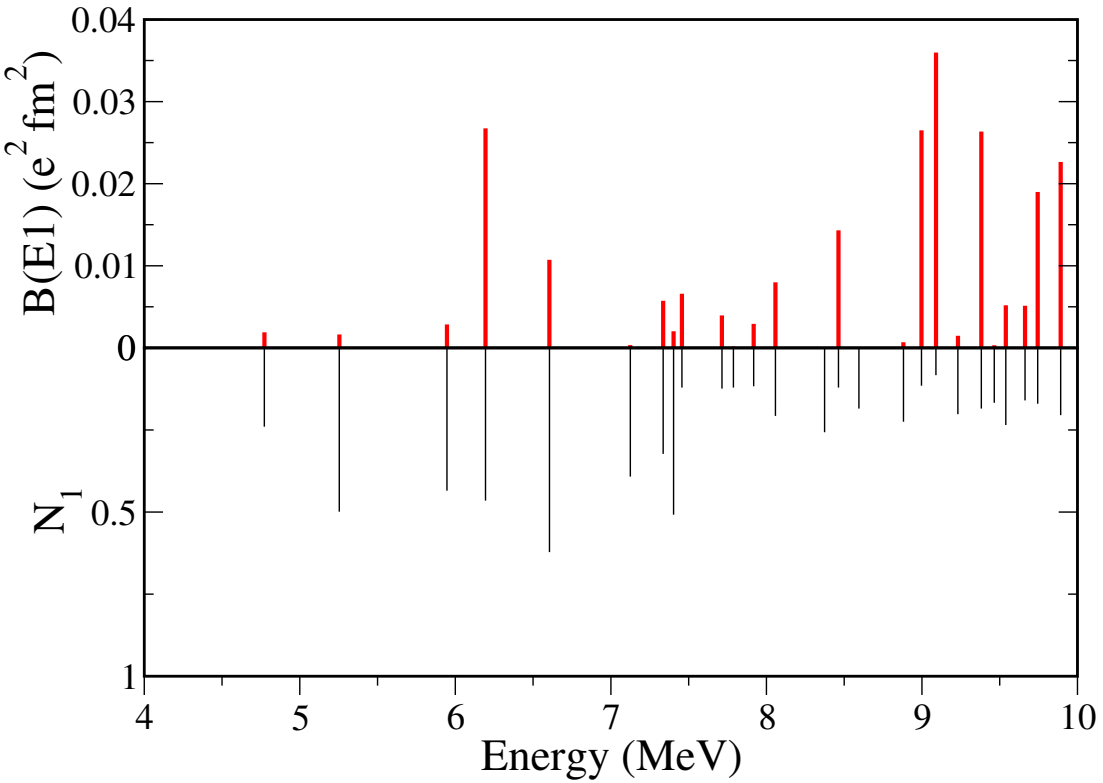

Coherence of the elementary $1p1h$ configurations in building the B(E1)

$$B^{\nu}(E\lambda) = |\sum_{ph}(X^{\nu}_{ph} - Y^{\nu}_{ph})F^{\lambda}_{ph}|^2 = |\sum_{ph} b^{\nu}_{ph}(E\lambda)|^2$$

where F^{λ}_{ph} are the multipole transition amplitudes of the operator

$$F = e\frac{N}{A}\sum_{i=1}^{Z} r_i Y_{10}(\Omega_i) - e\frac{Z}{A}\sum_{i=1}^{N} r_i Y_{10}(\Omega_i)$$

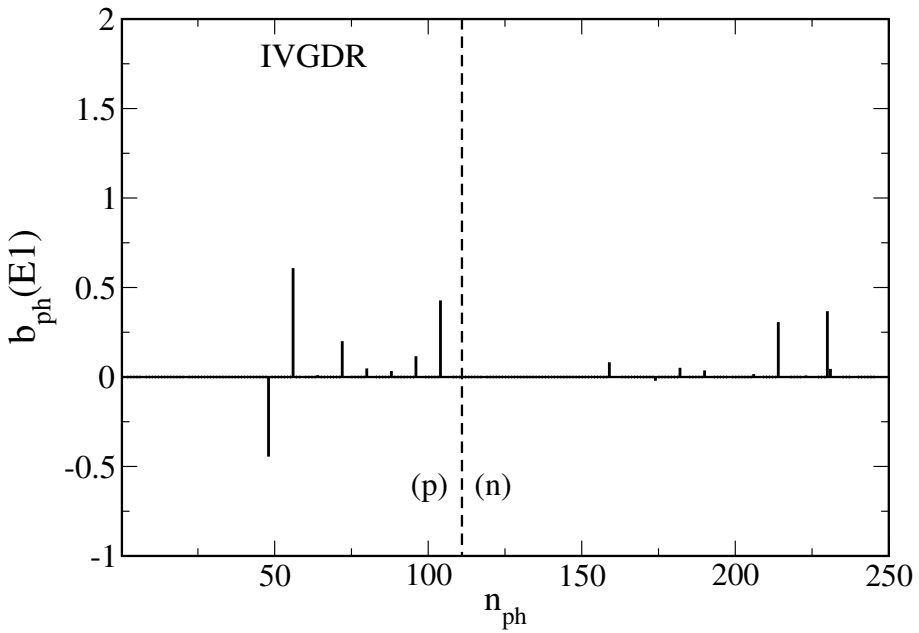

Coherence of the elementary $1p1h$ configurations in building the B(E1)

$$B^{\nu}(E\lambda) = |\sum_{ph}(X^{\nu}_{ph} - Y^{\nu}_{ph})F^{\lambda}_{ph}|^2 = |\sum_{ph} b^{\nu}_{ph}(E\lambda)|^2$$

where F^{λ}_{ph} are the multipole transition amplitudes of the operator

$$F = e\frac{N}{A}\sum_{i=1}^{Z} r_i Y_{10}(\Omega_i) - e\frac{Z}{A}\sum_{i=1}^{N} r_i Y_{10}(\Omega_i)$$

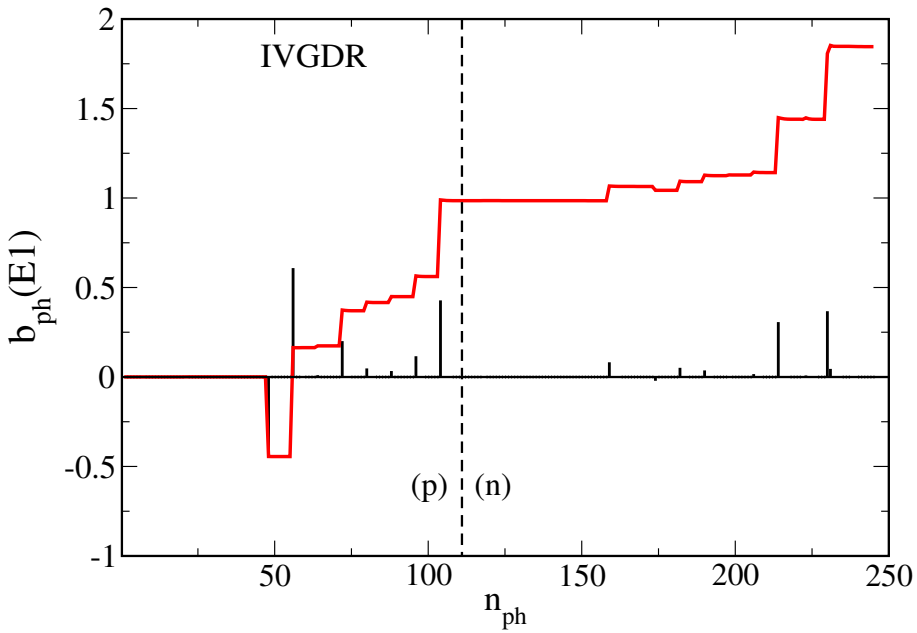

Collectivity: PDR case

ph conf.	$E = 6.19$ MeV			F^{λ}_{ph}
	E (MeV)	A_{ph}	$b_{ph}(E1)$	
$(1f_{7/2}, 1d_{5/2})^{\pi}$	11.732	0.156	−0.727	3.304
$(2p_{3/2}, 2s_{1/2})^{\pi}$	12.444	0.148	0.373	1.726
$(2p_{1/2}, 2s_{1/2})^{\pi}$	14.133	0.003	−0.043	−1.233
$(2p_{3/2}, 1d_{3/2})^{\pi}$	12.120	0.003	−0.015	0.451
$(2p_{1/2}, 1d_{3/2})^{\pi}$	13.809	0.073	0.166	1.053
$(1f_{5/2}, 1d_{3/2})^{\pi}$	13.867	0.018	0.250	2.756
$(2p_{3/2}, 1d_{5/2})^{\nu}$	15.683	0.000	0.012	1.410
$(2p_{3/2}, 2s_{1/2})^{\nu}$	11.773	0.015	−0.079	1.737
$(2p_{3/2}, 1d_{3/2})^{\nu}$	10.329	0.040	0.038	0.456
$(2p_{1/2}, 1d_{3/2})^{\nu}$	12.112	0.001	−0.016	1.084
$(1g_{9/2}, 1f_{7/2})^{\nu}$	11.364	0.003	−0.106	4.171
Partial Sum		0.461	−0.147	
Total Sum		0.465	−0.163	

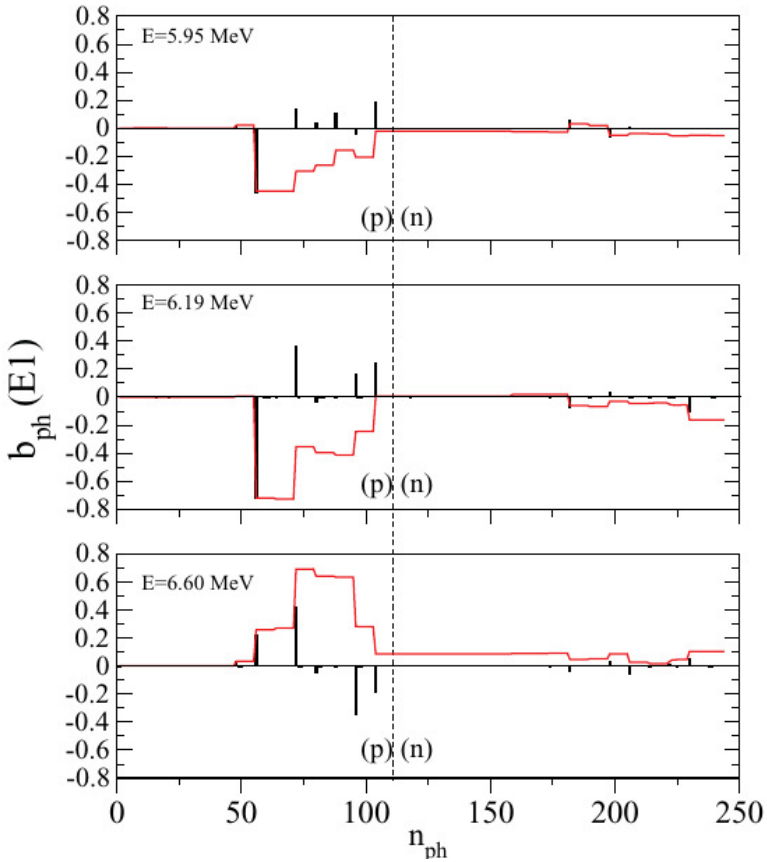

Collectivity: PDR case

ph conf.	$E = 6.19$ MeV			F^{λ}_{ph}
	E (MeV)	A_{ph}	$b_{ph}(E1)$	
$(1f_{7/2}, 1d_{5/2})^{\pi}$	11.732	0.156	−0.727	3.304
$(2p_{3/2}, 2s_{1/2})^{\pi}$	12.444	0.148	0.373	1.726
$(2p_{1/2}, 2s_{1/2})^{\pi}$	14.133	0.003	−0.043	−1.233
$(2p_{3/2}, 1d_{3/2})^{\pi}$	12.120	0.003	−0.015	0.451
$(2p_{1/2}, 1d_{3/2})^{\pi}$	13.809	0.073	0.166	1.053
$(1f_{5/2}, 1d_{3/2})^{\pi}$	13.867	0.018	0.250	2.756
$(2p_{3/2}, 1d_{5/2})^{\nu}$	15.683	0.000	0.012	1.410
$(2p_{3/2}, 2s_{1/2})^{\nu}$	11.773	0.015	−0.079	1.737
$(2p_{3/2}, 1d_{3/2})^{\nu}$	10.329	0.040	0.038	0.456
$(2p_{1/2}, 1d_{3/2})^{\nu}$	12.112	0.001	−0.016	1.084
$(1g_{9/2}, 1f_{7/2})^{\nu}$	11.364	0.003	−0.106	4.171
Partial Sum		0.461	−0.147	
Total Sum		0.465	−0.163	

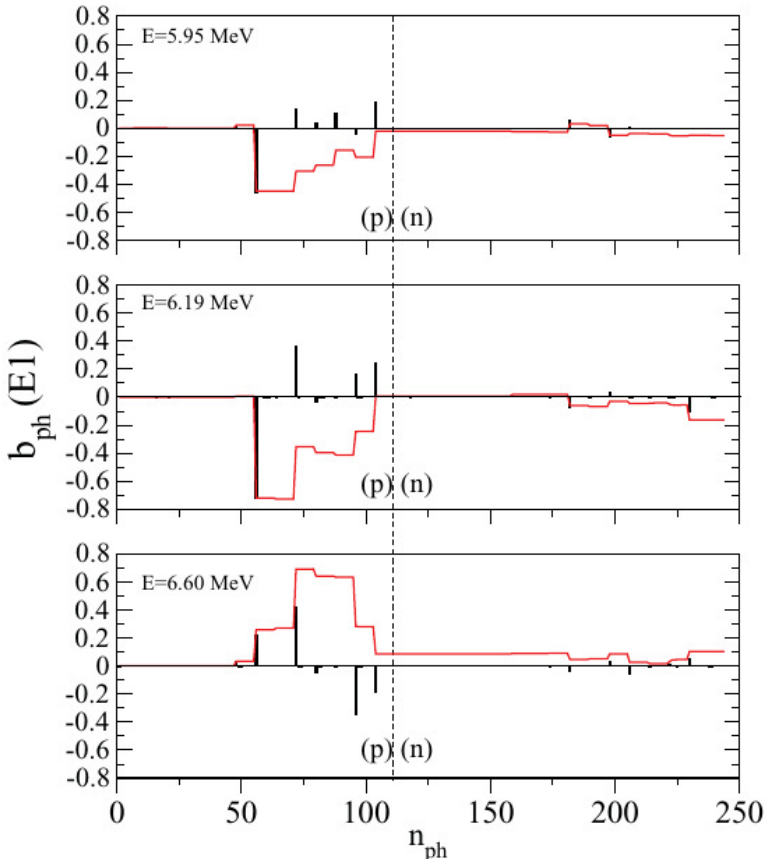

Several 1p-1h configurations participate but not coherently

SRPA, SSRPA vs Data

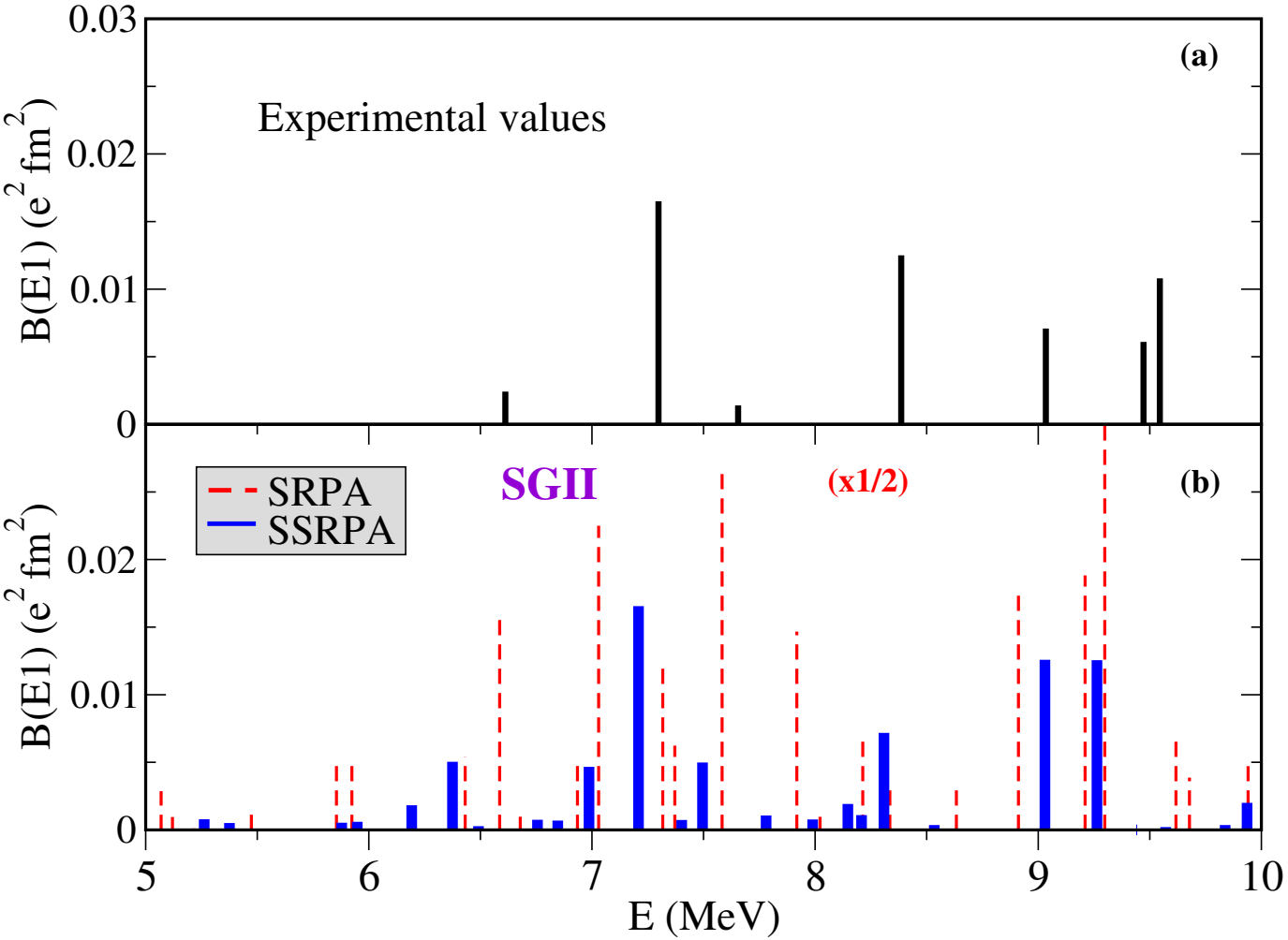

D. Gambacurta , M. Grasso , O. Vasseur, Physics Letters B 777 (2018) 163–168

Total $B(E1)$ and EWSRs (From 5 to 10 MeV)

	Exp	SRPA SGII	SSRPA SGII	SRPA SLy4	SSRPA SLy4
$\sum B(E1)$	0.068 $\pm$ 0.008	0.563	0.078	1.012	0.126
$\sum_i E_i B_i(E1)$	0.570 $\pm$ 0.062	4.618	0.621	8.795	1.062

Experimental and theoretical $\sum B(E1)$ in (e^2 fm^2) and $\sum_i E_i B_i(E1)$ in (MeV e^2 fm^2) summed between 5 and 10 MeV.
From D. G., M. Grasso , O. Vasseur, Physics Letters B 777 (2018) 163–168

Total $B(E1)$ and EWSRs (From 5 to 10 MeV)

	Exp	SRPA SGII	SSRPA SGII	SRPA SLy4	SSRPA SLy4
$\sum B(E1)$	0.068 $\pm$ 0.008	**0.563**	**0.078**	1.012	0.126
$\sum_i E_i B_i(E1)$	0.570 $\pm$ 0.062	**4.618**	**0.621**	8.795	1.062

Experimental and theoretical $\sum B(E1)$ in (e^2 fm^2) and $\sum_i E_i B_i(E1)$ in (MeV e^2 fm^2) summed between 5 and 10 MeV.
From D. G., M. Grasso , O. Vasseur, Physics Letters B 777 (2018) 163–168

Low-energy dipole states in ^{68}Ni

Experimental measurements: relativistic Coulomb excitations at GSI

- (I) O. Wieland et al., Phys. Rev. Lett. 102, 092502 (2009): strength centered at around 11 MeV with a contribution of 5% to the EWSR
- (II) D.M. Rossi et al., Phys. Rev. Lett. 111, 242503 (2013): strength centered at around 9.55 MeV with a contribution of 2.8% to the EWSR
- The discrepancy in the value of the centroid was explained as a possible 'energy–dependent branching ratio'

Low-energy dipole states in ^{68}Ni

Experimental measurements: relativistic Coulomb excitations at GSI

- (I) O. Wieland et al., Phys. Rev. Lett. 102, 092502 (2009): strength centered at around 11 MeV with a contribution of 5% to the EWSR
- (II) D.M. Rossi et al., Phys. Rev. Lett. 111, 242503 (2013): strength centered at around 9.55 MeV with a contribution of 2.8% to the EWSR
- The discrepancy in the value of the centroid was explained as a possible 'energy–dependent branching ratio'
- Isoscalar excitation on ^{12}C target @ LNS: peak located around 10 MeV with a contribution of 10% to the EWSR (N.S. Martorana et al., Phys. Lett. B 782, 112 (2018))

Low-energy dipole states in ^{68}Ni, theoretical study

- SSRPA versus RPA strength distributions
- Comparison with experimental data
- Transition densities of some selected (low-lying) peaks are analyzed
- We estimate beyond–mean–field (BMF) on the symmetry energy (J) and on its slope (L)
- M. Grasso and DG Phys. Rev. 101, 064314 (2020)

Low-energy dipole states in ^{68}Ni

Low-energy dipole states in ^{68}Ni, theoretical study

- SSRPA versus RPA strength distributions
- Comparison with experimental data
- Transition densities of some selected (low-lying) peaks are analyzed
- **We estimate beyond–mean–field (BMF) on the symmetry energy (J) and on its slope (L)**
- M. Grasso and DG Phys. Rev. 101, 064314 (2020)

BMF effects estimation: employed linear correlations

- Percentage of (PDR) EWSR and L:
  A. Klimkiewicz et al., Phys. Rev. C 76, 051603 (R) (2007); A. Carbone et al., Phys. Rev. C 81, 041301 (R) (2010)
- L and neutron–skin thickness:
  M. Centelles et al., Phys. Rev. Lett. 102, 122502 (2009); M. Wardaet al.,, Phys. Rev. C 80, 024316 (2009)
- Neutron–skin thickness and electric dipole polarizability times the J coefficient: X. Roca-Maza et al. Phys. Rev. C 92, 064304 (2015).

Low-energy dipole states in ^{68}Ni: RPA and SSRPA with SGII interaction

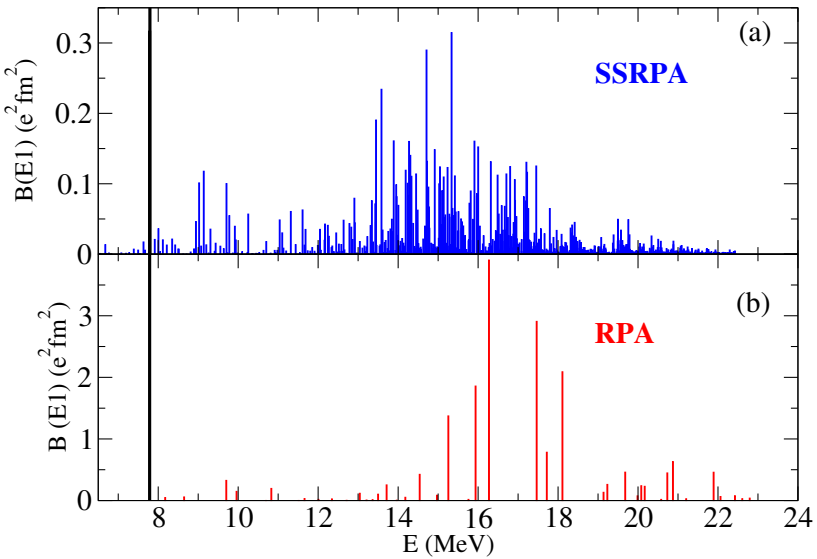

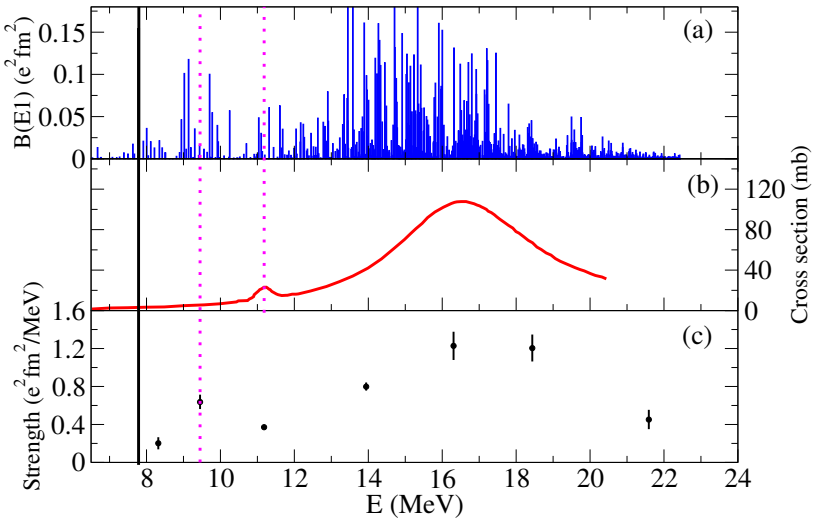

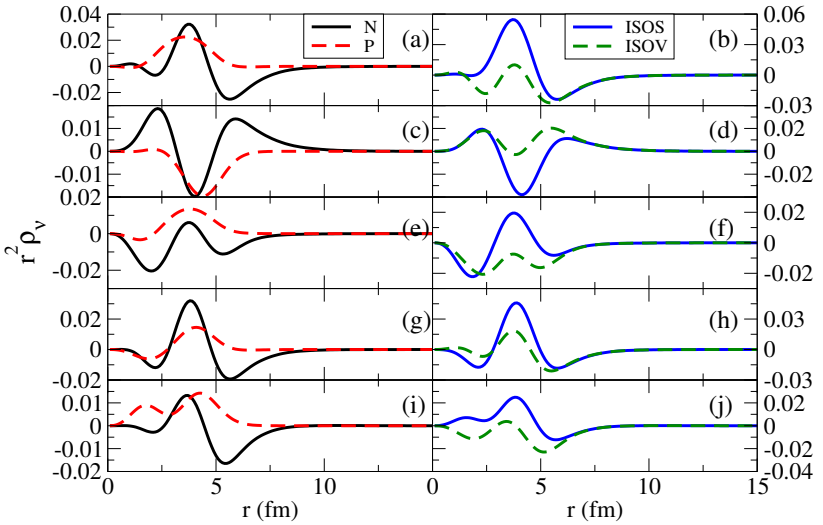

Peaks located at 9.14 ((a) and (b)), 9.70 ((c) and (d)), 10.25 ((e) and (f)), 11.10 ((g) and (h)), and 11.31 ((i) and (j))

Low-energy dipole states in ^{68}Ni: RPA and SSRPA with SGII interaction

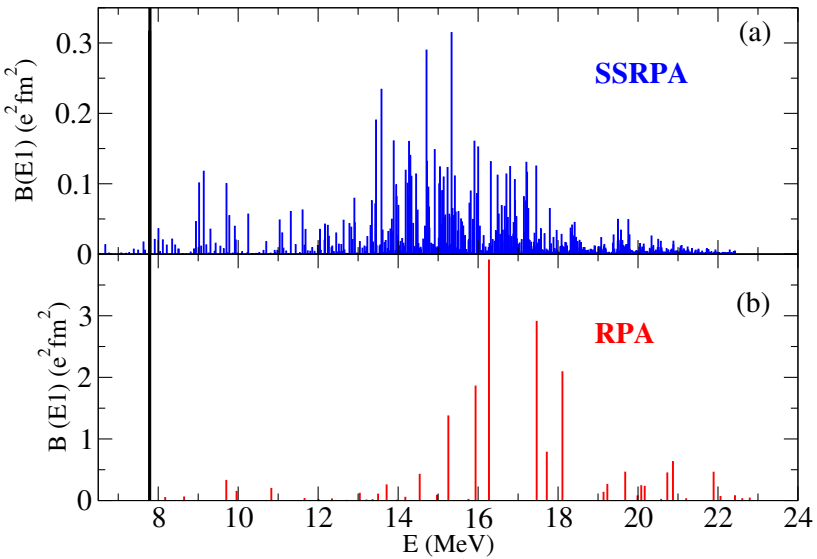

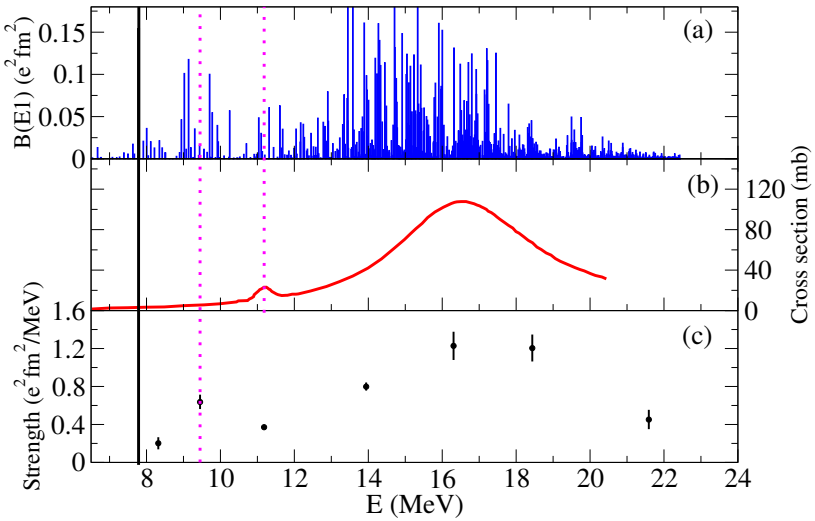

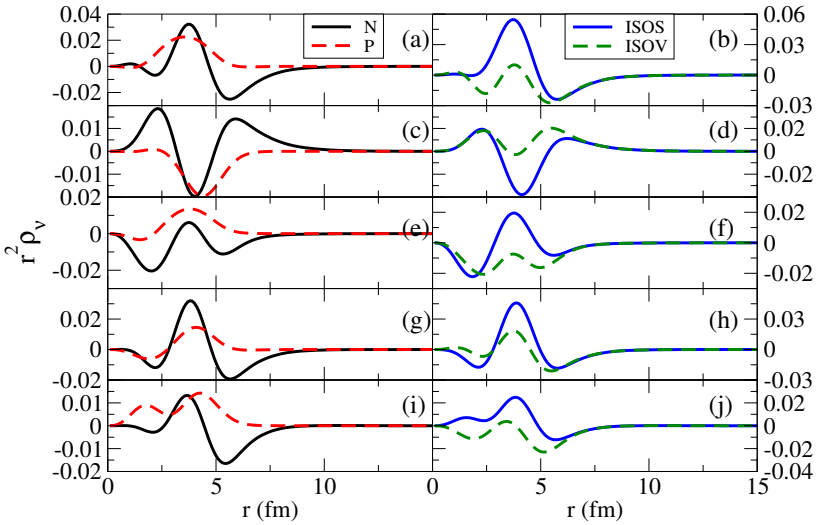

Peaks located at 9.14 ((a) and (b)), 9.70 ((c) and (d)), 10.25 ((e) and (f)), 11.10 ((g) and (h)), and 11.31 ((i) and (j))

Skyrme	J (MeV)	L (MeV)
SIII	28.16	9.90
SGII	26.83	37.70
SkI4	29.50	60.00
SkI3	34.27	100.49

Beyond-mean-field effects on the symmetry energy and its slope

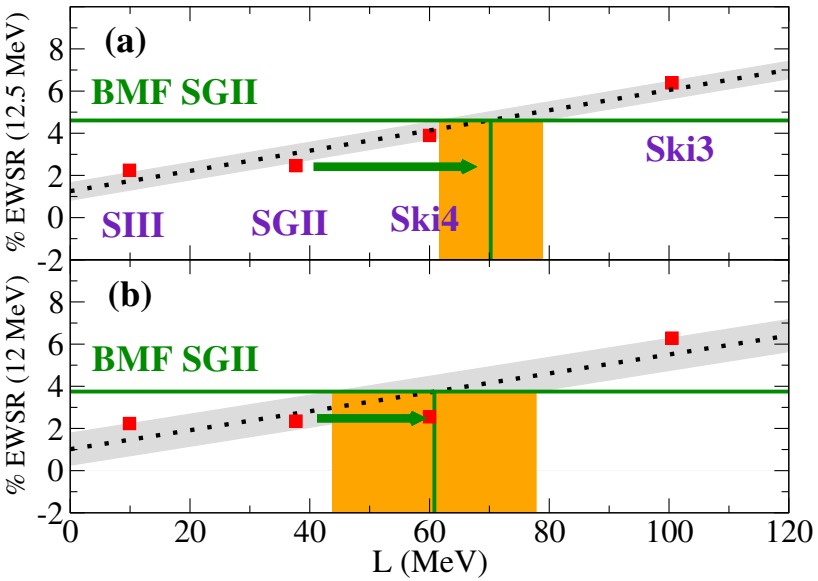

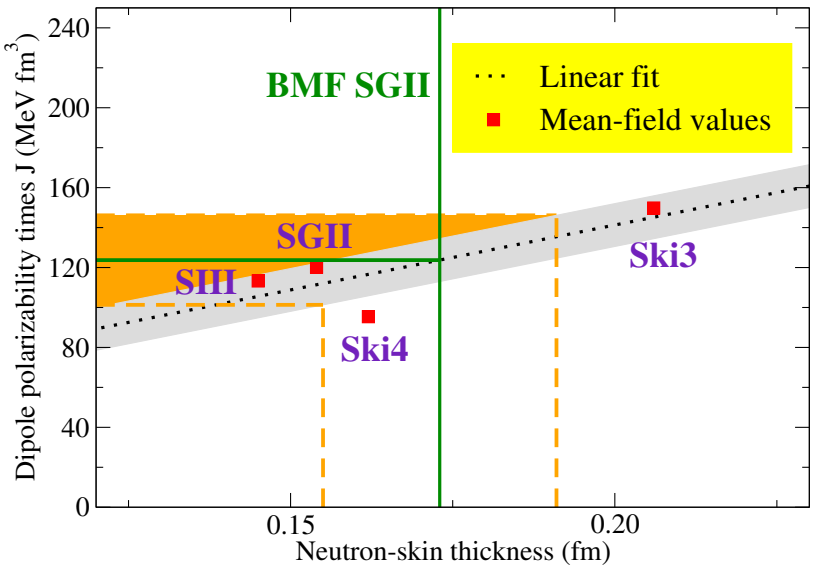

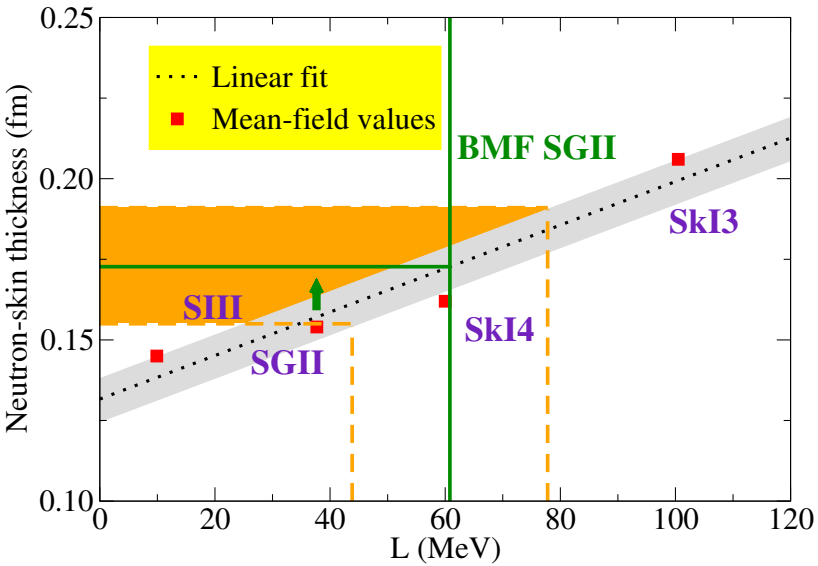

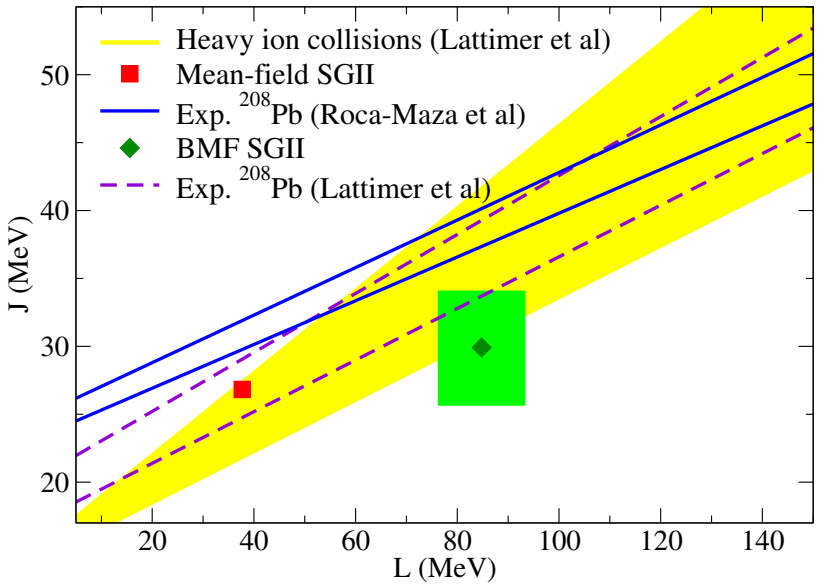

Beyond-mean-field effects on the symmetry energy and its slope

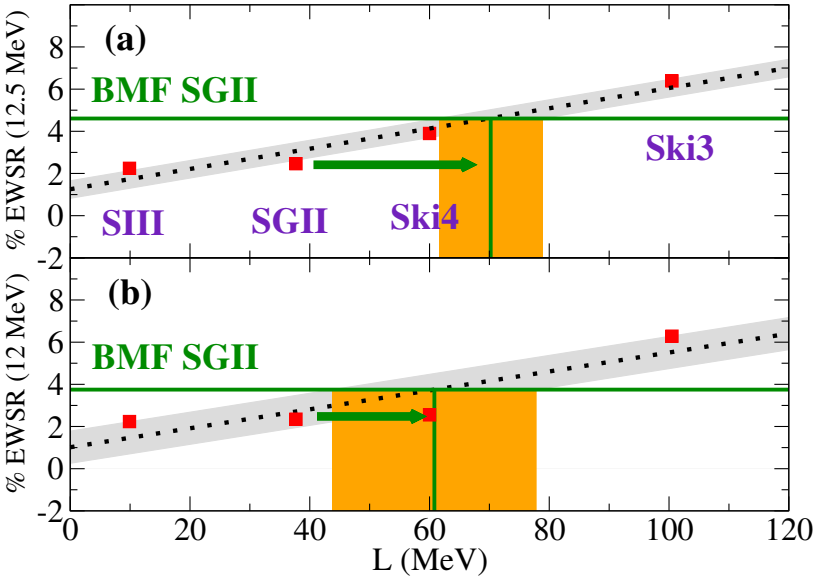

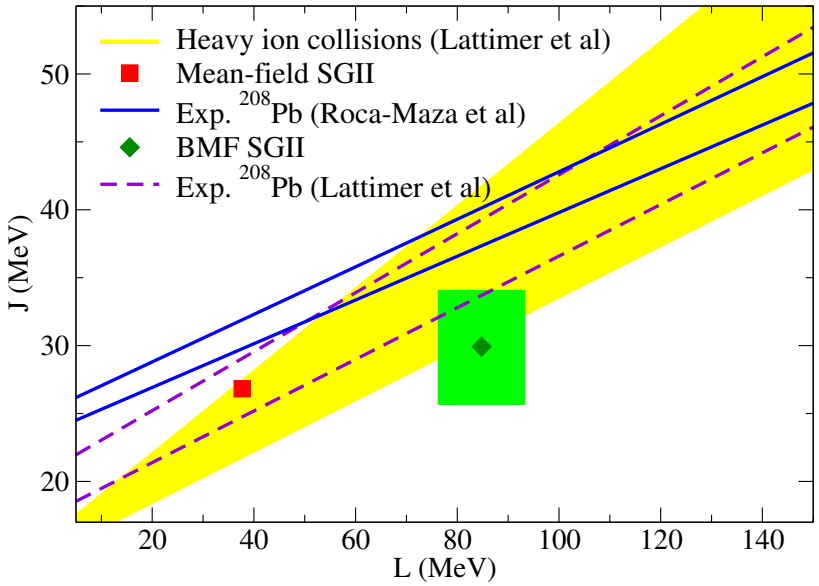

	L (MeV)	Δr_{np} (fm)	J (MeV)
Mean field	37.70	0.154	26.83
BMF	60.815 $\pm$ 16.982	0.173 $\pm$ 0.018	27.617 $\pm$ 5.004

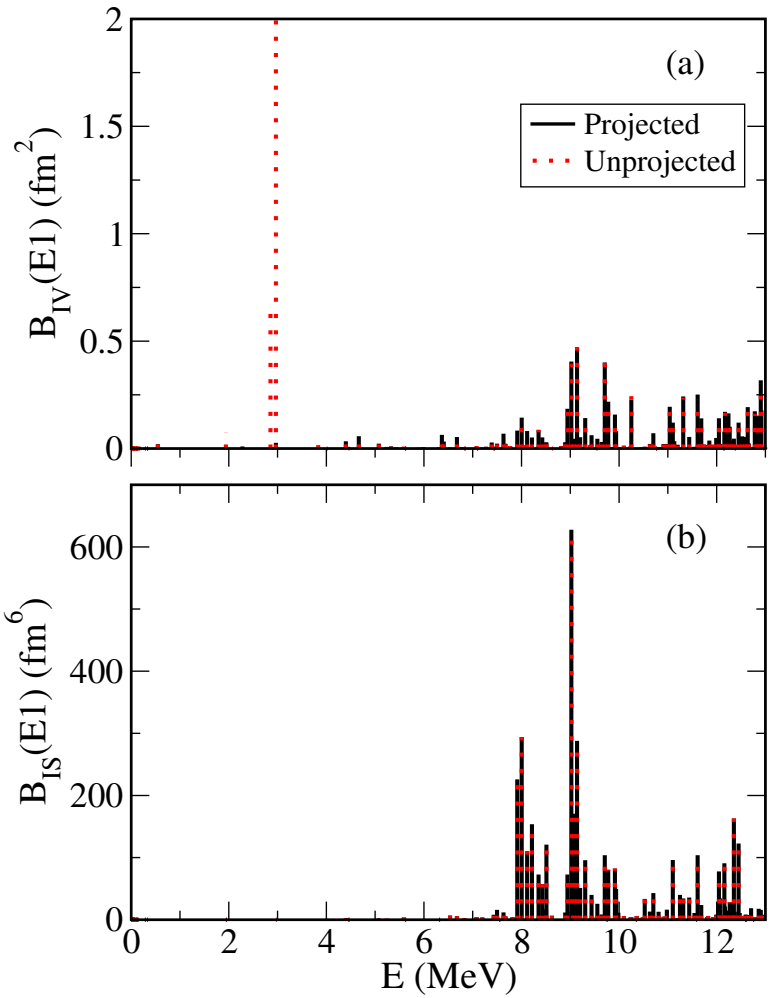

Spurious components

- Procedure proposed in X. Roca-Maza et al. Phys. Rev. C 85, 024601 (2012)
- Projection out of spurios components (*á posteriori*)
- See Frantisek Knapp's talk, for a (more rigorous) treatment of spurious components in SRPA-like approaches

Monopole response in RPA and SSRPA

- Evolution of the response in Ca isotopes from ^{40}Ca to ^{60}Ca
- $N = 20$ isotones : ^{40}Ca, ^{36}S and ^{34}Si
- The case of ^{68}Ni

The key-points of our study

- Soft monopole modes driven by neutron excitations
- Not only at the surface of the nucleus but over its entire volume
- Properties are discussed as a function of the isospin asymmetry
- More details: DG, M. Grasso and O. Sorlin, PRC 100, 014317 (2019)

Monopole strength distribution in Ca isotopes

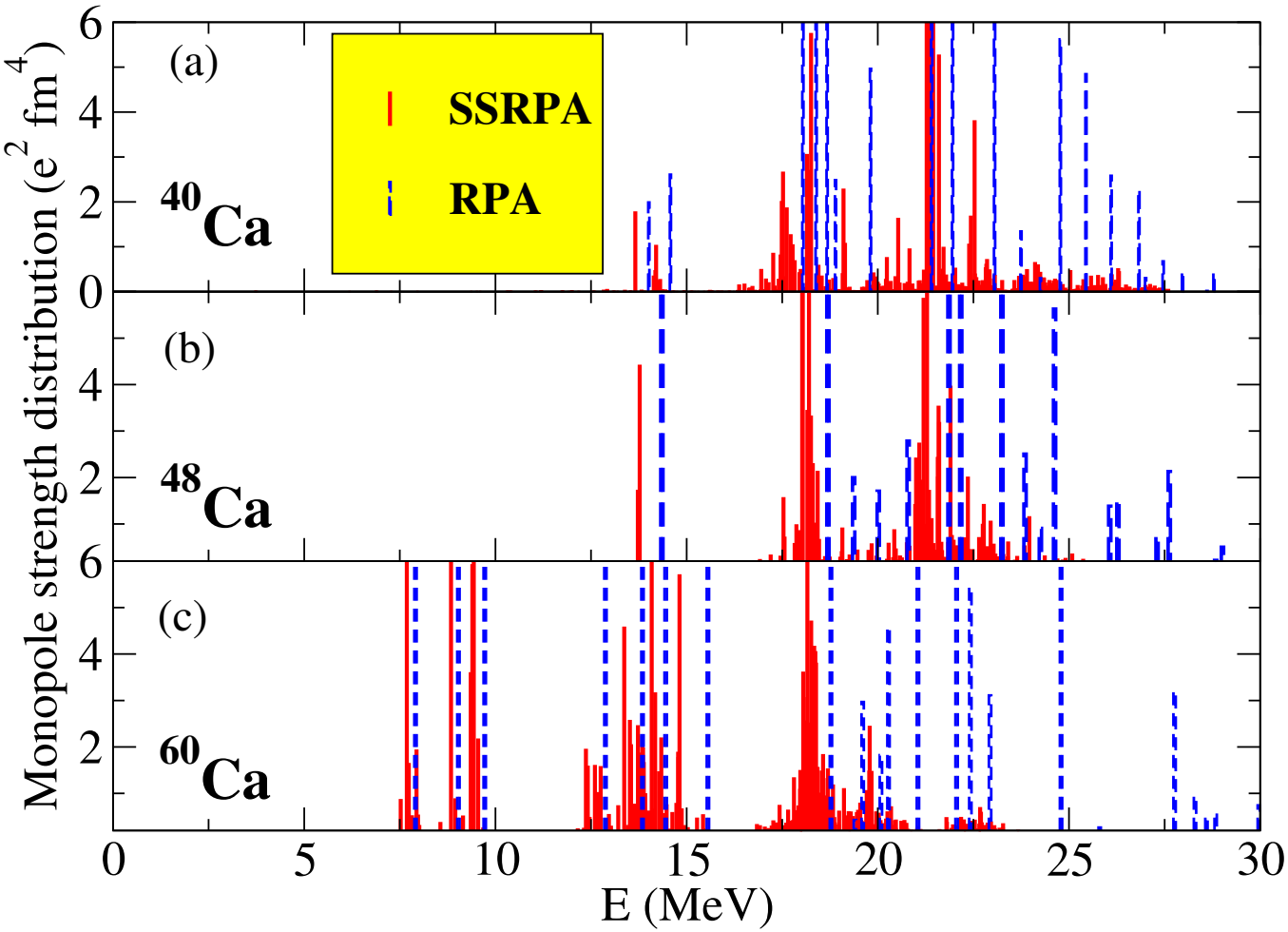

(a) Monopole strength distribution computed with RPA (dashed blue bars) and SSRPA (full red bars) for ^{40}Ca; (b) Same as in (a) but for ^{48}Ca; (c) Same as in (a) but for ^{60}Ca.

Comparison with data from Y.-W. Lui, et al., PRC 83, 044327 (2011)

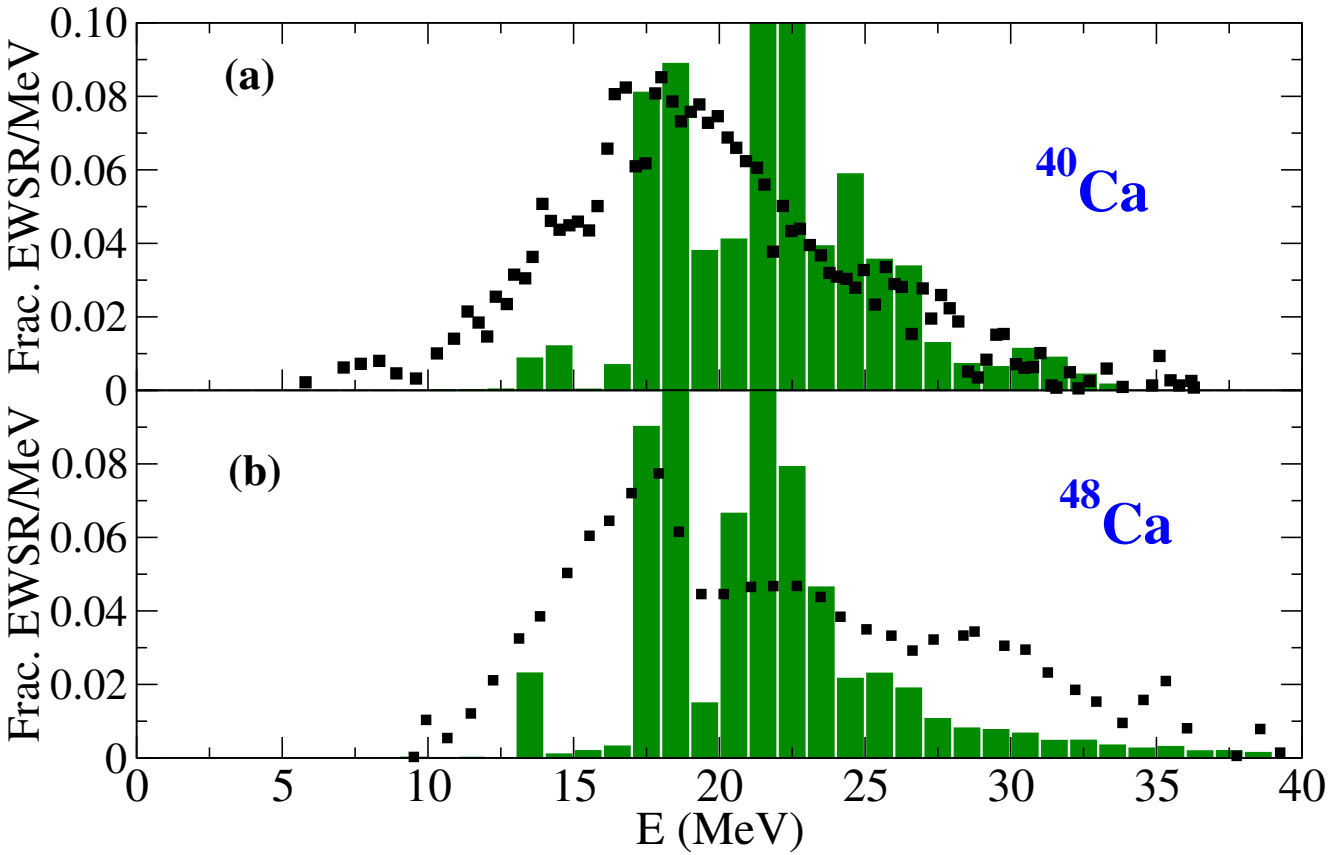

(a) Black squares: experimental results ; green bars: SSRPA predictions for ^{40}Ca; (b) Same as in (a) but for ^{48}Ca.

Centroids (MeV)

^{40}Ca: 21.3 (RPA), 20.7 (SSRPA), 18.3 (Exp)

^{48}Ca: 20.7 (RPA), 20.4 (SSRPA), 19.0 (Exp)

Transition densities in ^{40}Ca

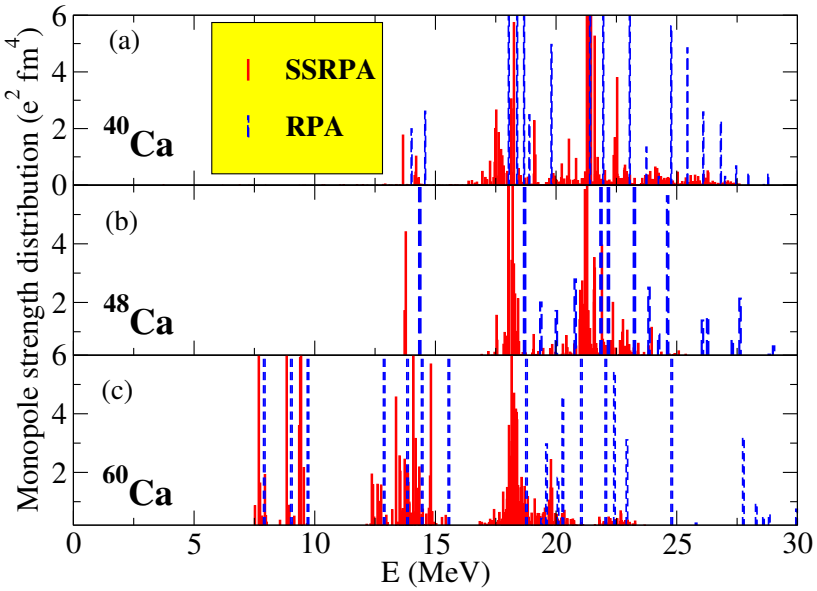

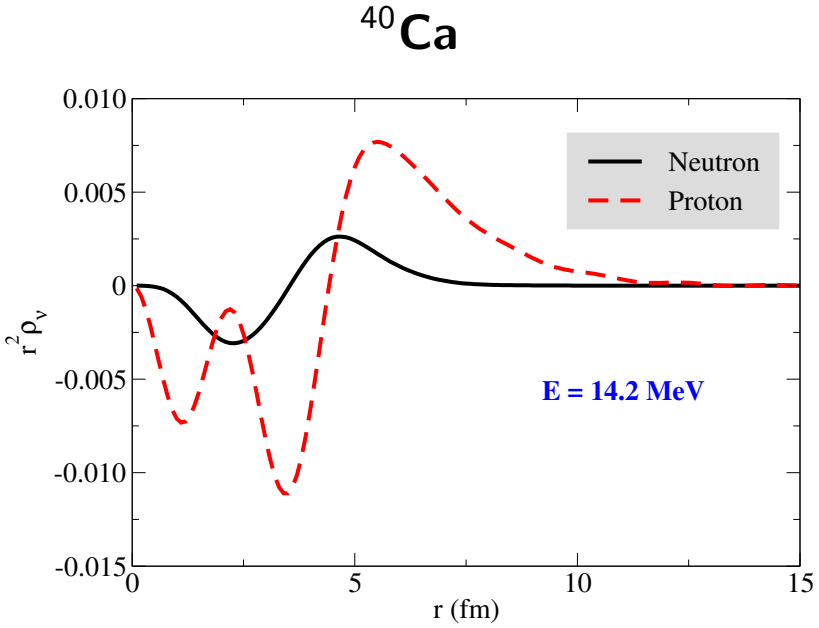

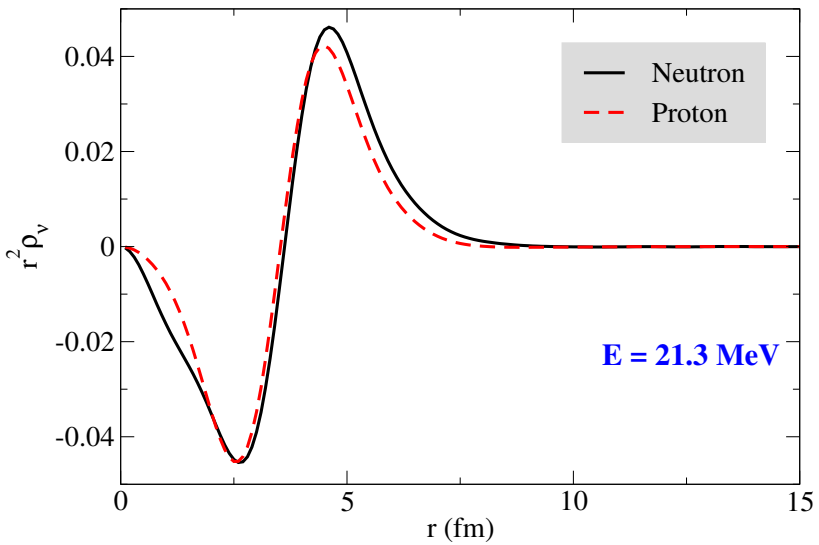

Transition densities in ^{48}Ca

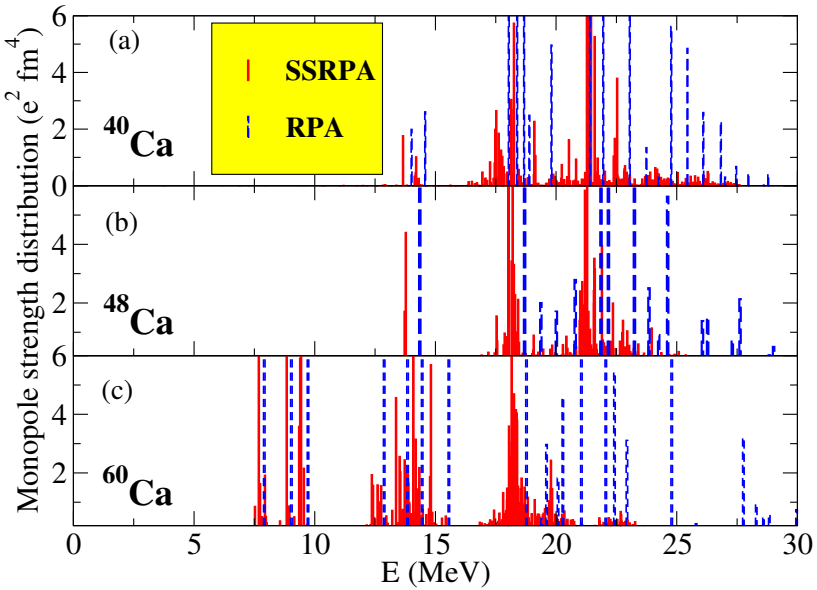

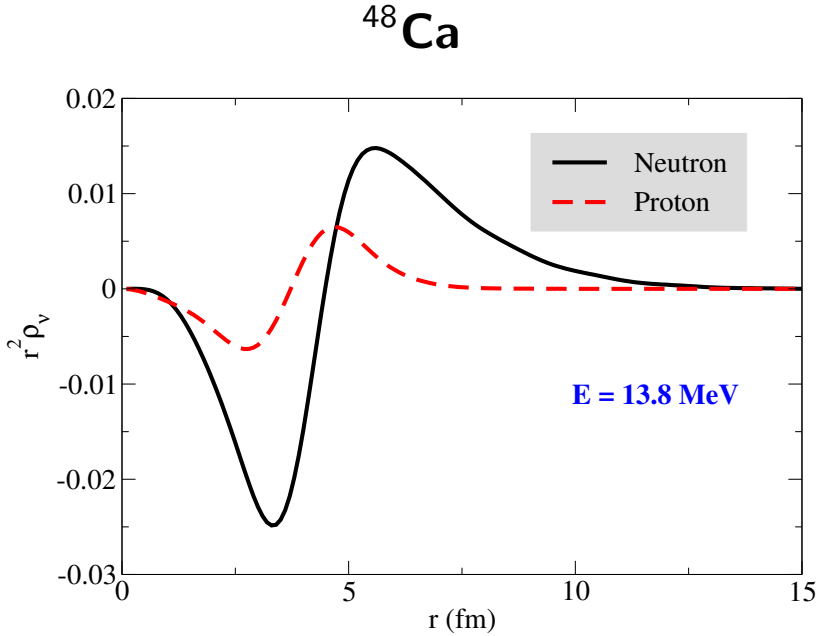

Transition densities in ^{60}Ca

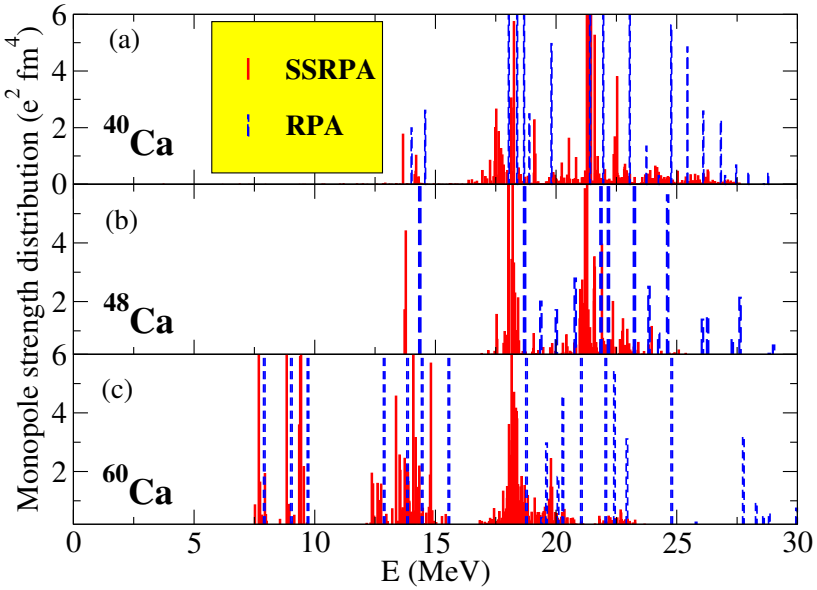

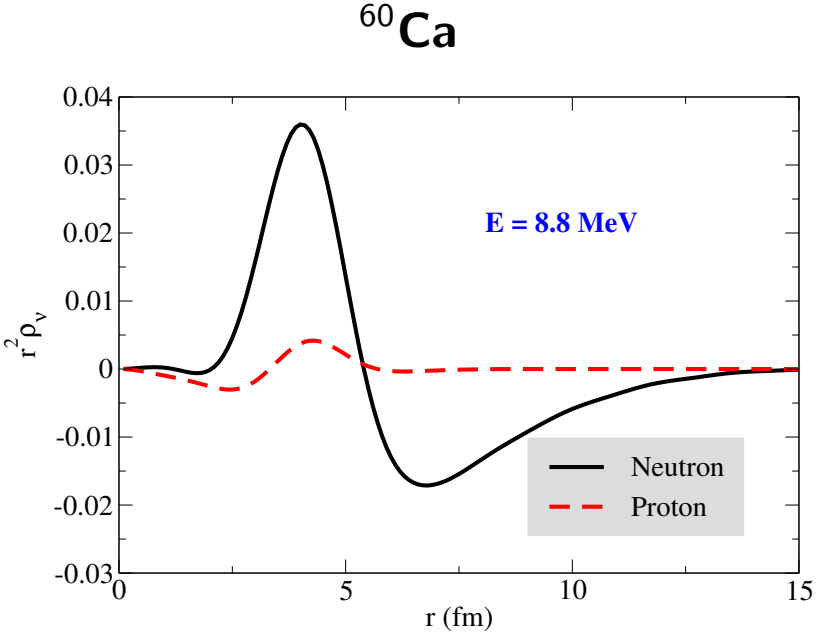

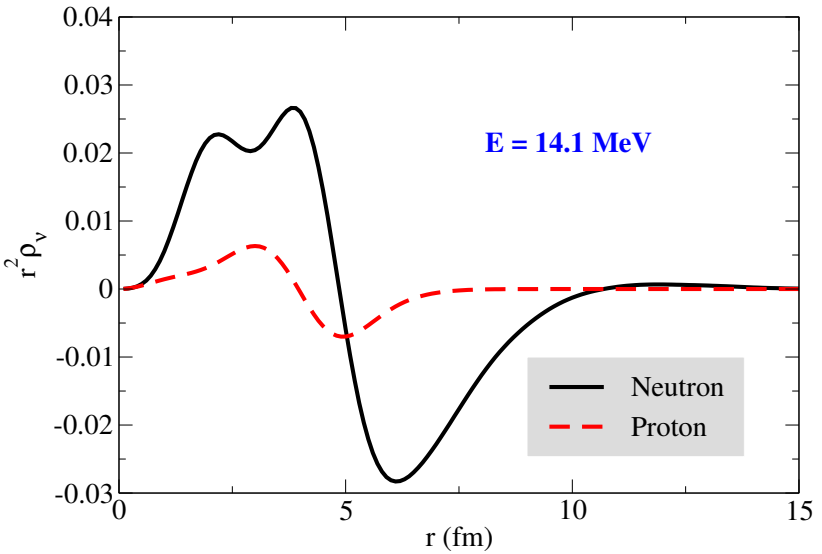

Monopole strength distribution in ^{34}Si and ^{36}S

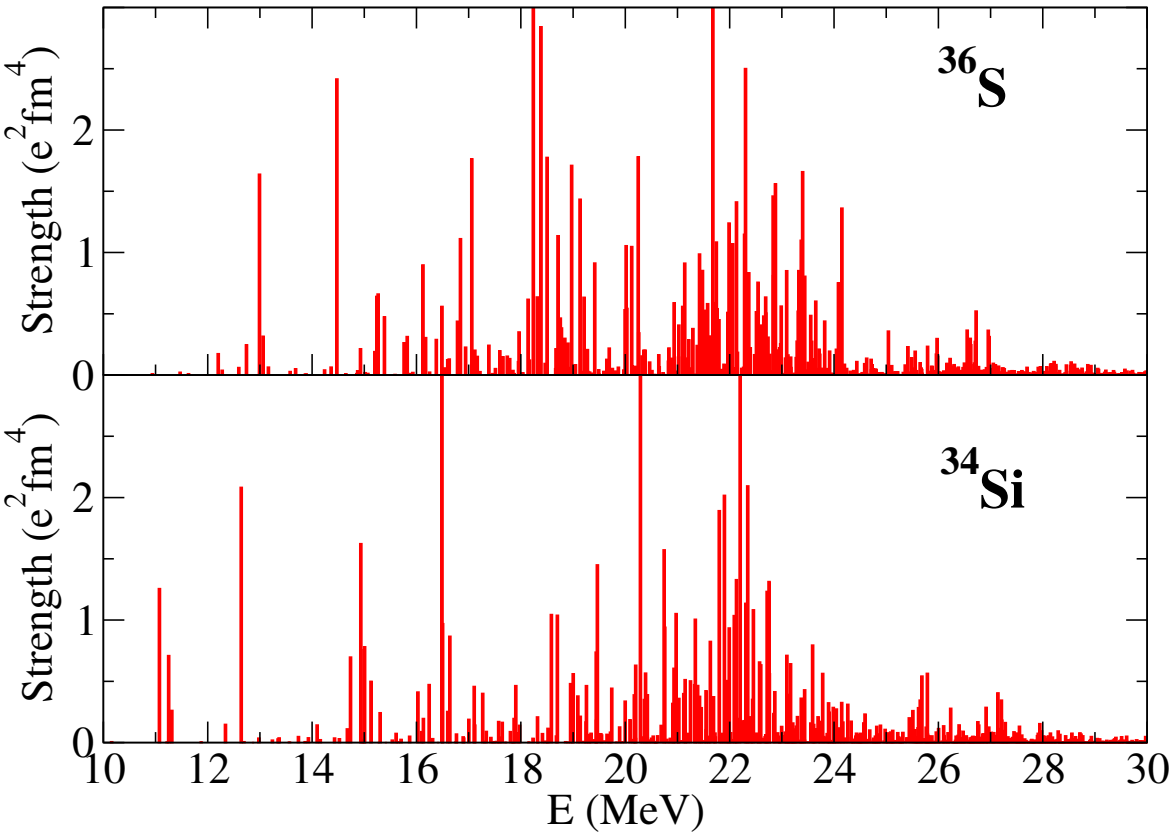

Monopole isoscalar strength distributions calculated for the nuclei ^{36}S (a) and ^{34}Si (b).

Transition densities in ^{34}Si and ^{36}S

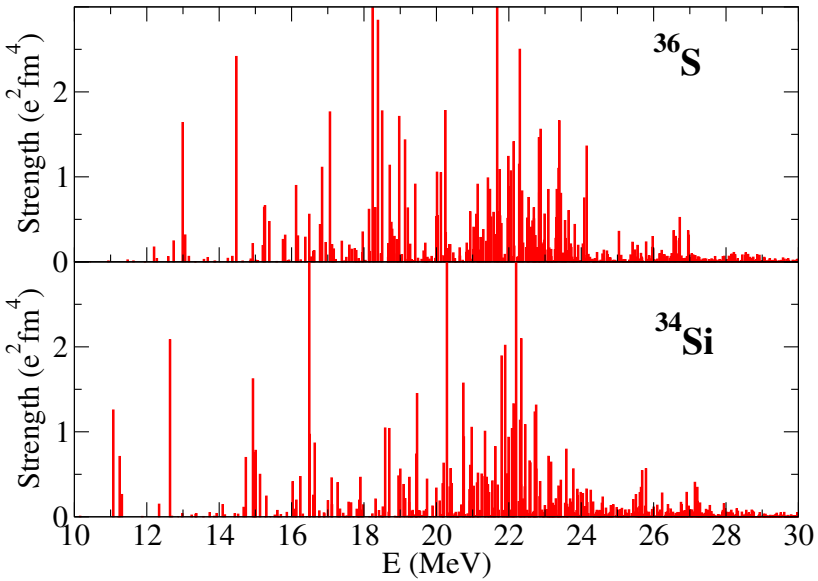

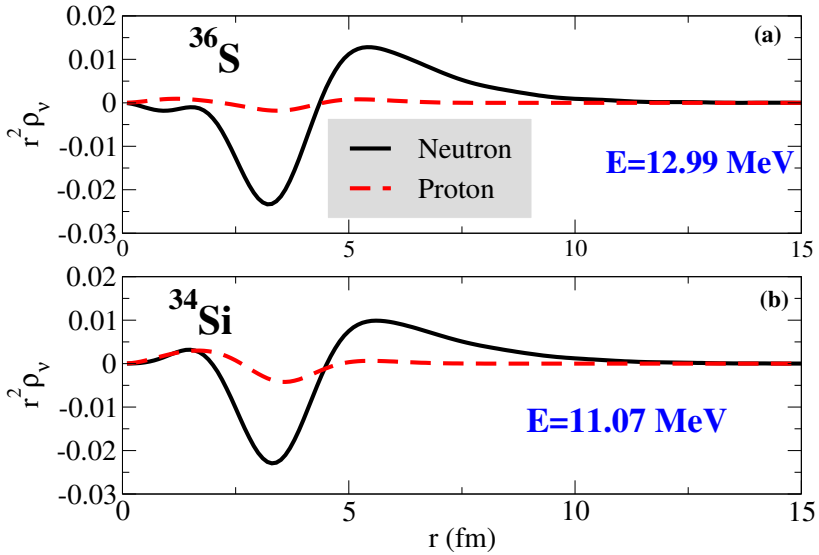

Composition of the peak located at 11.07 (12.99) MeV for ^{34}Si (^{36}S).

^{34}Si	1p1h 54 %	2p2h 46 %
	$[\nu 2d_{3/2}, \nu 1d_{3/2}]^{J=0}$	$[[\pi 3p_{1/2}, \nu 3f_{7/2}]^{J_p=3}[\pi 1d_{5/2}, \nu 2s_{1/2}]^{J_h=3}]^{J=0}$ $[[\pi 4p_{1/2}, \nu 1f_{5/2}]^{J_p=2}[\pi 1d_{5/2}, \nu 2s_{1/2}]^{J_h=2}]^{J=0}$ $[[\pi 4p_{1/2}, \nu 1f_{5/2}]^{J_p=3}[\pi 1d_{5/2}, \nu 2s_{1/2}]^{J_h=3}]^{J=0}$ $[[\pi 6s_{1/2}, \nu 2d_{3/2}]^{J_p=2}[\pi 1d_{5/2}, \nu 1d_{3/2}]^{J_h=2}]^{J=0}$ $[[\pi 6s_{1/2}, \nu 2d_{5/2}]^{J_p=2}[\pi 1d_{5/2}, \nu 1d_{3/2}]^{J_h=2}]^{J=0}$ $[[\pi 3d_{3/2}, \nu 3s_{1/2}]^{J_p=2}[\pi 1d_{5/2}, \nu 1d_{3/2}]^{J_h=2}]^{J=0}$ $[[\pi 3d_{3/2}, \nu 2d_{5/2}]^{J_p=1}[\pi 1d_{5/2}, \nu 1d_{3/2}]^{J_h=1}]^{J=0}$ $[[\pi 3d_{3/2}, \nu 2d_{5/2}]^{J_p=2}[\pi 1d_{5/2}, \nu 1d_{3/2}]^{J_h=2}]^{J=0}$
^{36}S	1p1h 52 %	2p2h 48 %
	$[\nu 2d_{3/2}, \nu 1d_{3/2}]^{J=0}$	$[[\pi 3d_{3/2}, \nu 4d_{3/2}]^{J_p=2}[\pi 1d_{5/2}, \nu 1d_{3/2}]^{J_h=2}]^{J=0}$ $[[\pi 4d_{3/2}, \nu 4s_{1/2}]^{J_p=2}[\pi 2s_{1/2}, \nu 1d_{3/2}]^{J_h=2}]^{J=0}$ $[[\pi 4d_{3/2}, \nu 5s_{1/2}]^{J_p=1}[\pi 2s_{1/2}, \nu 1d_{3/2}]^{J_h=1}]^{J=0}$ $[[\pi 4d_{3/2}, \nu 4d_{3/2}]^{J_p=2}[\pi 2s_{1/2}, \nu 1d_{3/2}]^{J_h=2}]^{J=0}$ $[[\pi 4d_{3/2}, \nu 2d_{5/2}]^{J_p=1}[\pi 2s_{1/2}, \nu 1d_{3/2}]^{J_h=1}]^{J=0}$

Transition densities in ^{68}Ni

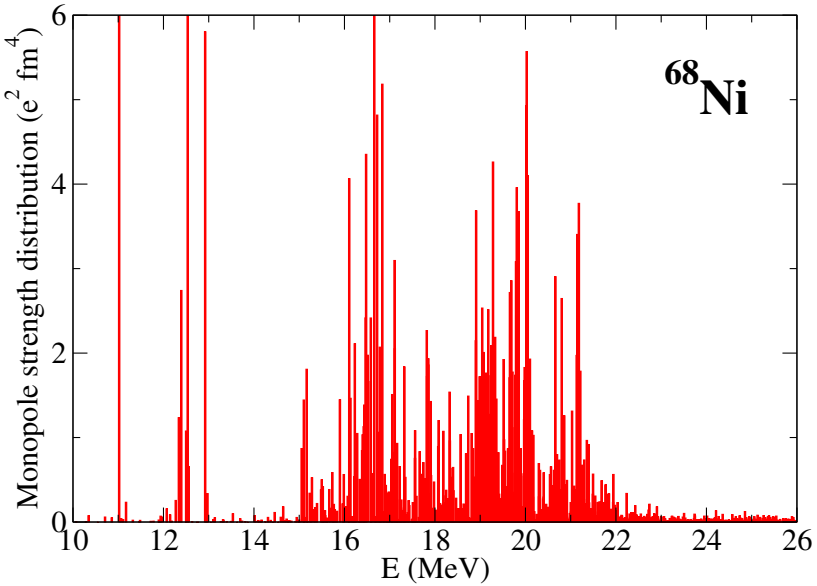

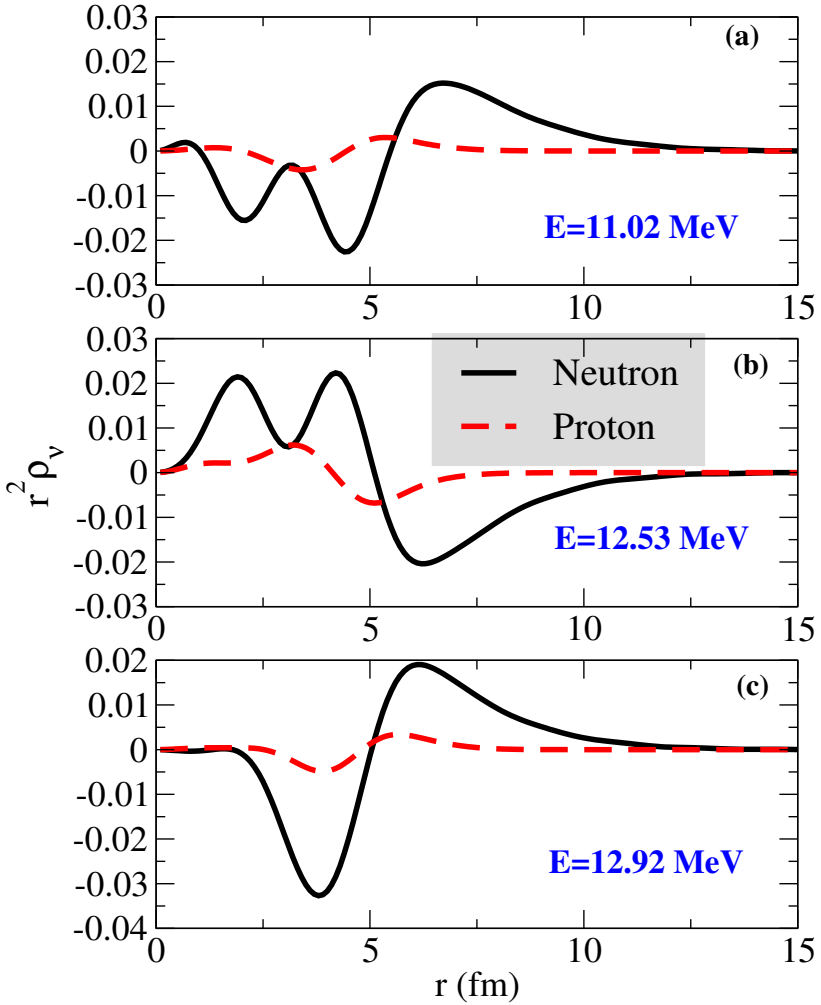

Low–energy states contribution to the EWSR.

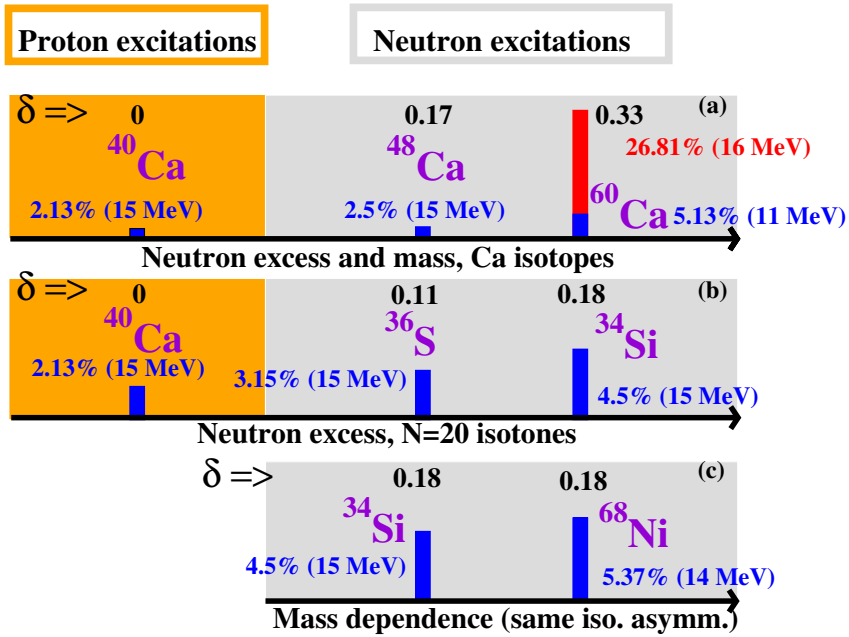

Percentages of the EWSR versus isospin asymmetry $\delta = (N - Z)/A$.
(a) Ca isotopes: evolution as a function of the neutron excess and the mass;
(b) $N = 20$ isotones: evolution as a function of the neutron excess;
(c) Evolution as a function of the mass for two nuclei with the same isospin asymmetry, ^{34}Si and ^{68}Ni.

Low–energy states contribution to the EWSR.

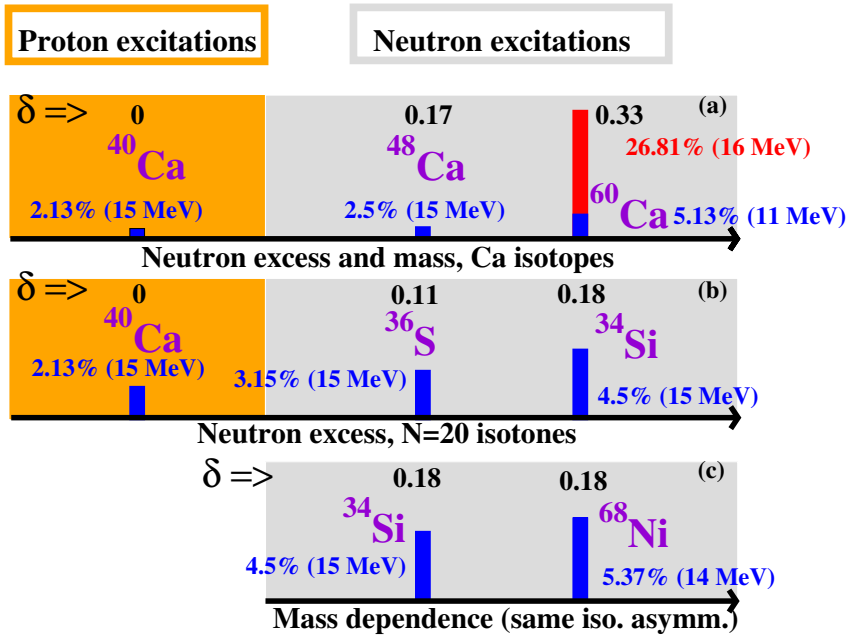

Percentages of the EWSR versus isospin asymmetry $\delta = (N - Z)/A$.
(a) Ca isotopes: evolution as a function of the neutron excess and the mass;
(b) $N = 20$ isotones: evolution as a function of the neutron excess;
(c) Evolution as a function of the mass for two nuclei with the same isospin asymmetry, ^{34}Si and ^{68}Ni.

Soft monopole states: single particle nature, neutron driven, extend in the whole volume (not only surface)

Recent extension to the charge exchange (CE) case

Subtracted SRPA (SSRPA) for CE excitations

- Extension of the SSRPA to the treatment of CE excitations
- First applications to ^{48}Ca (lightest double-β emitter) and ^{78}Ni in Ref [1]
- More applications (^{14}C, ^{22}O, ^{90}Zr and ^{132}Sn) in Ref [2]

More details in:

[1] D.Gambacurta, M. Grasso, J. Engel, Phys. Rev. Lett. 125, 212501 (2020)
[2] D.Gambacurta and M. Grasso, Phys. Rev. C 105, 014321, (2022)

The quenching problem

- Computed GT matrix elements **are larger** than the experimental ones.
- The problem is "cured" by **quenching** the strength by $q \sim 0.7$ or using effective axial constant g_A (~ 1) instead of the "bare" value ~ 1.27.

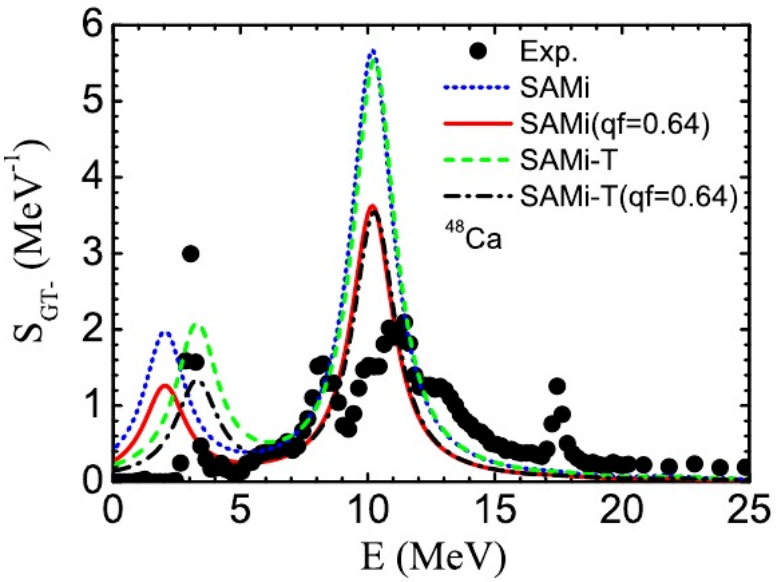

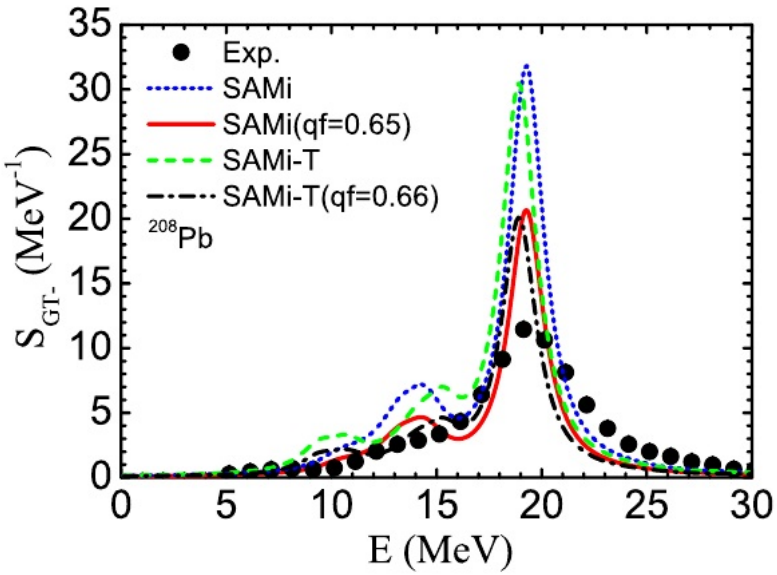

$$qf = \frac{\sum_{E_x=0}^{E_x(\max)} B(GT : E_x)_{\text{expt}}}{\sum_{E_x=0}^{E_x(\max)} B(GT)_{\text{calc}}}$$

Li-Gang Cao , Shi-Sheng Zhang, and H. Sagawa, PHYSICAL REVIEW C 100, 054324 (2019)

Skyrme-RPA calculations

The quenching problem

- Computed GT matrix elements **are larger** than the experimental ones.
- The problem is "cured" by **quenching** the strength by $q \sim 0.7$ or using effective axial constant g_A (~ 1) instead of the "bare" value ~ 1.27.

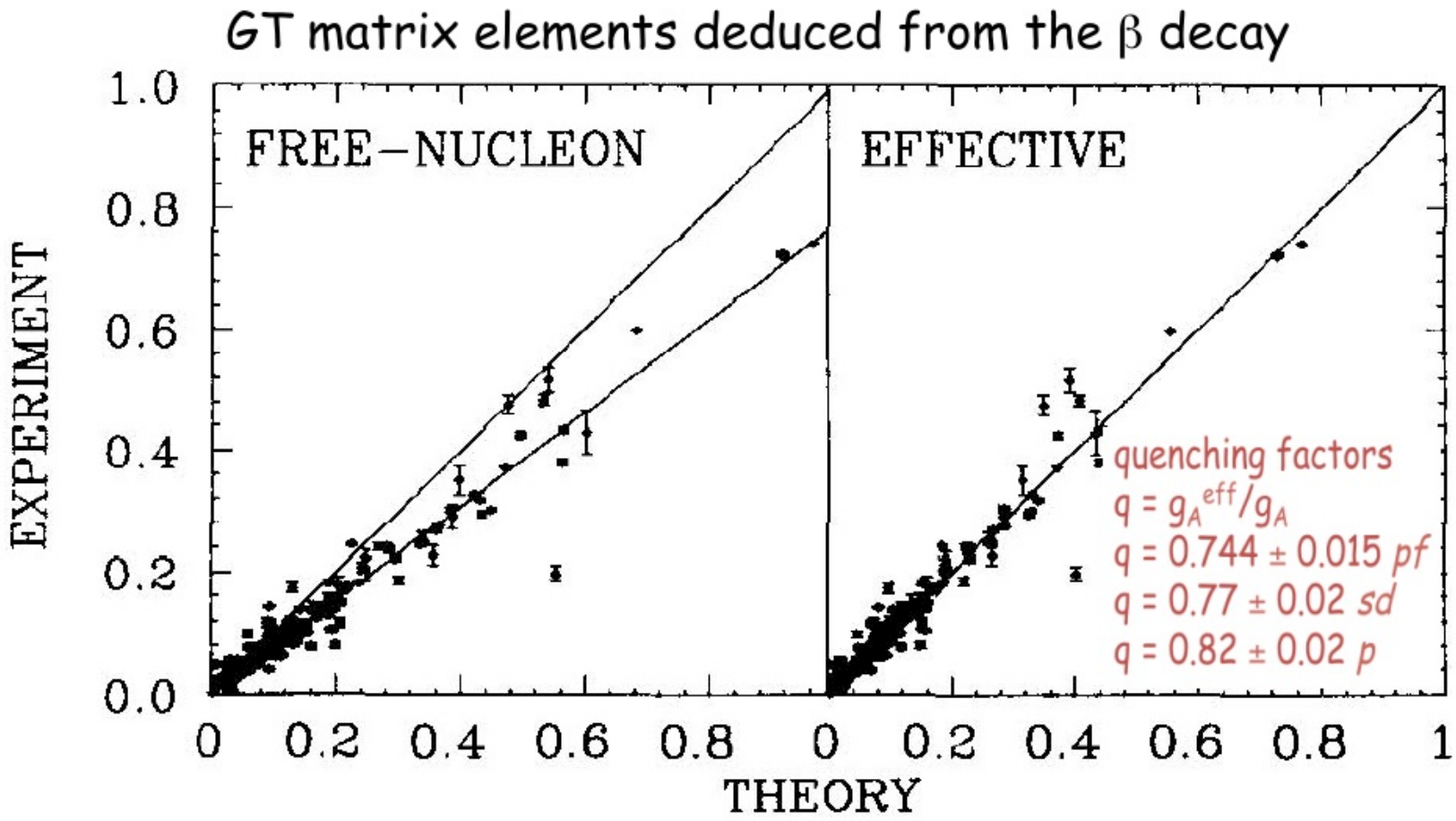

(from Brown & Wildenthal, Ann.Rev.Nucl. Part.Sci.**38**,(1988)29)

GT$^-$ Strength Distribution ^{48}Ca, SGII interaction

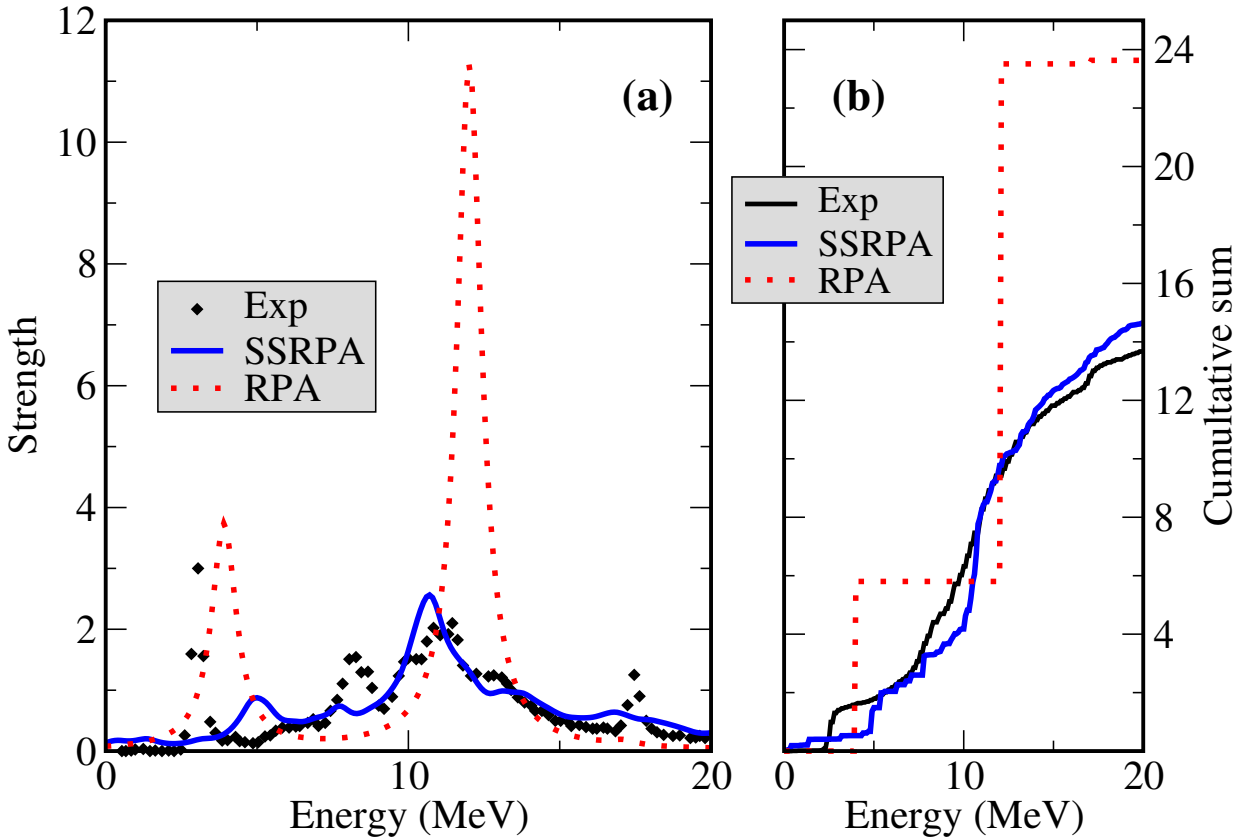

(a) GT$^-$ strength in RPA and SSRPA compared with (GT$^-$ plus IVSM) data.
(b) Cumulative strengths up to 20 MeV.
Data from: K. Yako *et al.*, Phys. Rev. Lett. 103, 012503 (2009)
From D.Gambacurta, M. Grasso, J. Engel, Phys. Rev. Lett. 125, 212501 (2020)

GT^- Strength Distribution ^{48}Ca

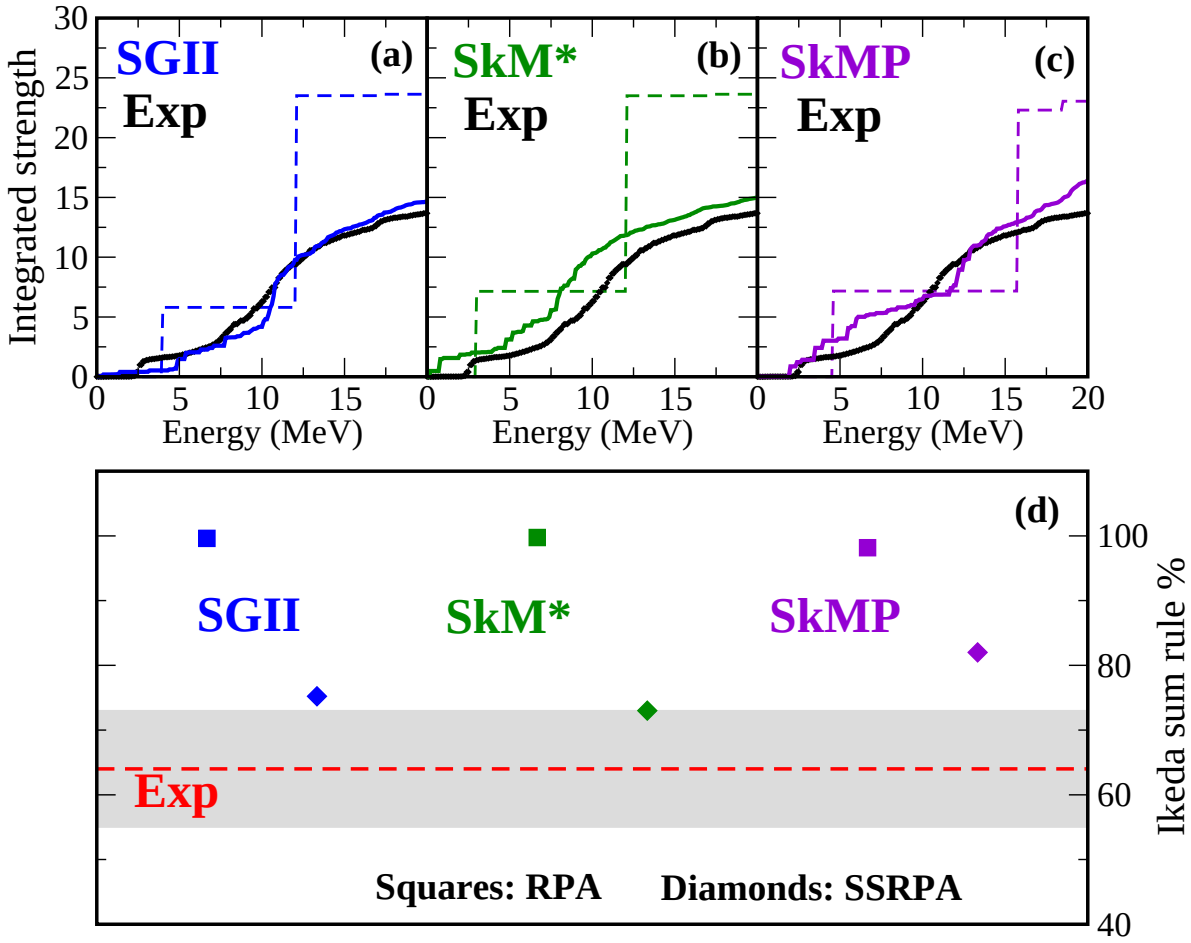

(a), (b), (c) Strengths integrated up to 20 MeV with different parameterizations.

(d) RPA and SSRPA percentages of the Ikeda sum rule below 30 MeV compared with the experimental one.

From D.Gambacurta, M. Grasso, J. Engel, Phys. Rev. Lett. 125, 212501 (2020)

GT$^-$ Strength Distribution and β-decay half-life ^{78}Ni

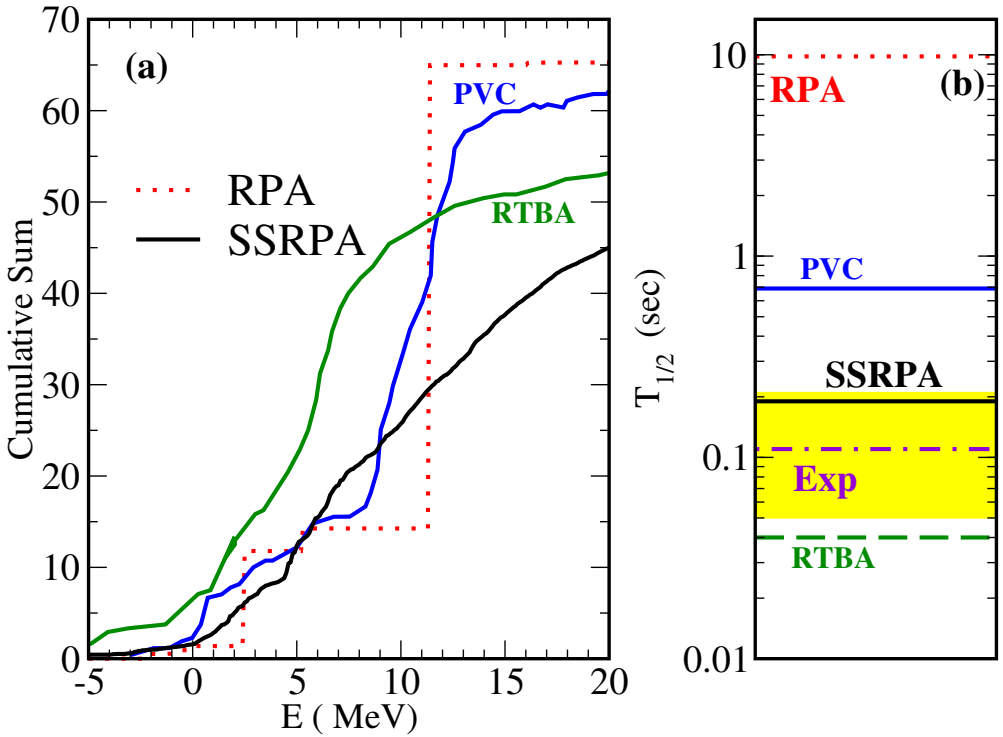

(a) Cumulative sum for the nucleus ^{78}Ni within the SSRPA, PVC and RTBA models;
(b) β-decay half-life for ^{78}Ni. **No quenching, bare** $g_a = 1.27$**;**
Data from: P. T. Hosmer *et al.* Phys. Rev. Lett. 94, 112501 (2005)
PVC: Y. F. Niu, G. Coló and E. Vigezzi, Phys. Rev. C 90, 054328 (2014)
RTBA:C. Robin and E. Litvinova, Phys. Rev. C 98, 051301(R), 2018

From D.Gambacurta, M. Grasso, J. Engel, Phys. Rev. Lett. 125, 212501 (2020)

GT^- Strength Distribution ^{90}Zr and ^{132}Sn, interaction dependence

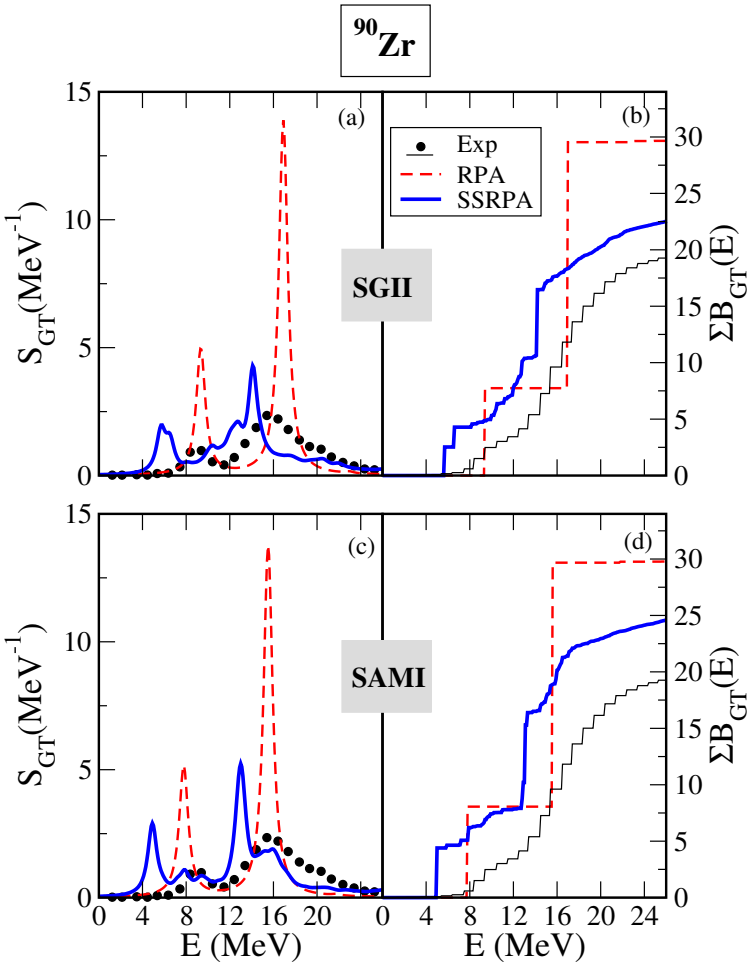

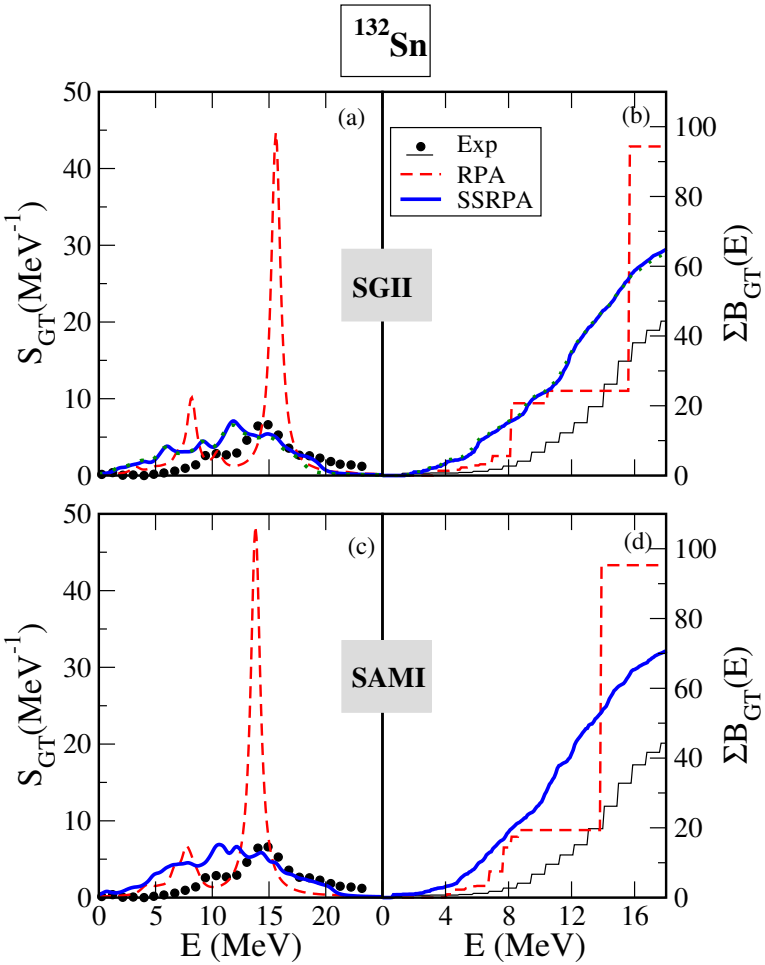

GT^- Strength Distribution ^{90}Zr and ^{132}Sn, interaction dependence

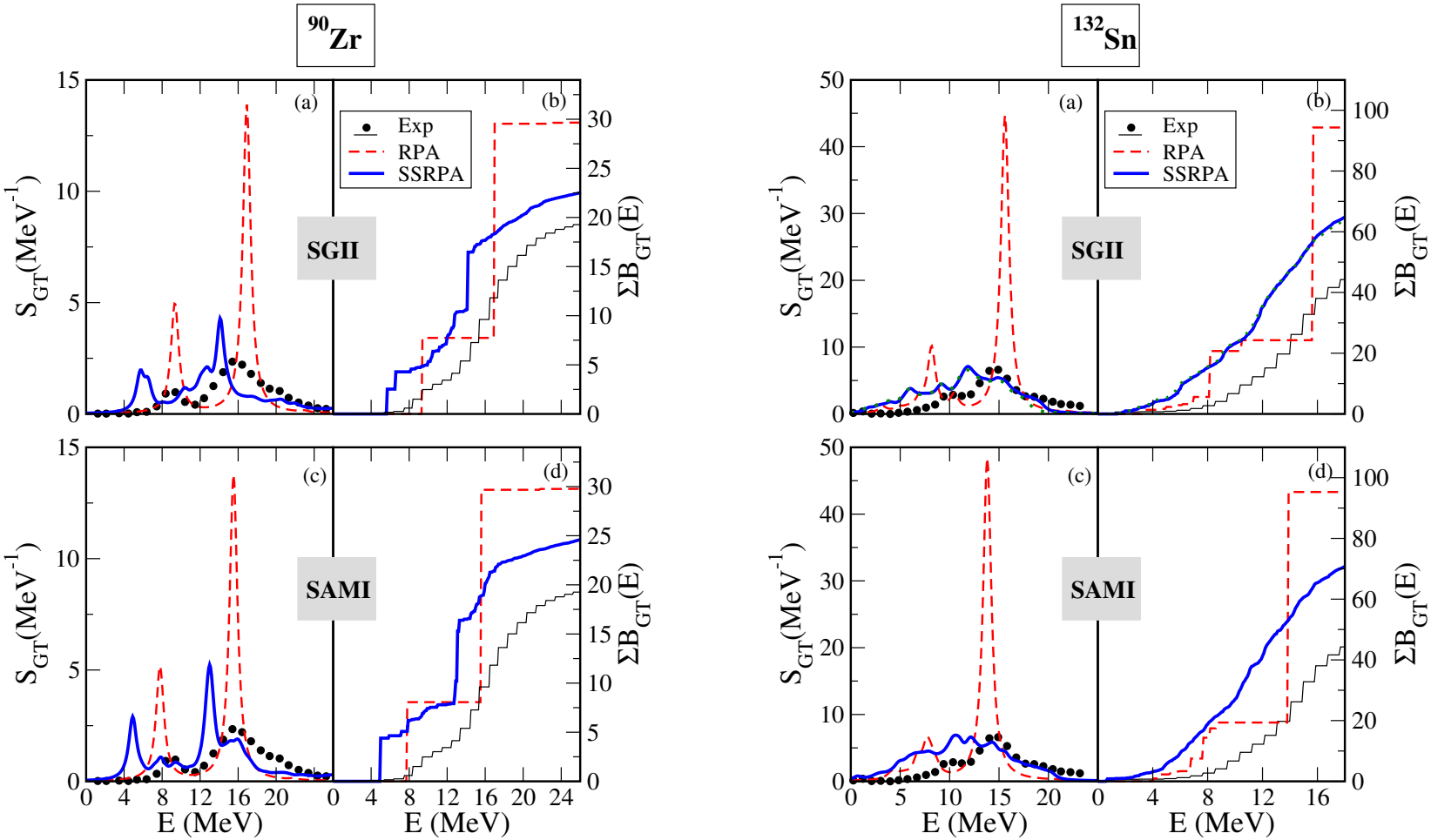

Other sources of queenching may be needed ...

D.Gambacurta and M. Grasso, Phys. Rev. C 105, 014321, (2022)

Conclusions

- The SSRPA provides a richer and more general description of nuclear excitations (2p-2h configurations $\Rightarrow$ fragmentation and width)
- Subtraction is crucial to improve the agreement with data
- Dipole response in ^{48}Ca
- Dipole response ^{68}Ni $\Rightarrow$ BMF effects on the symmetry energy (J) and its slope (L): qualitative estimation (BMF effects increase both J and L)
- Soft monopole excitations: "neutron-driven" excitations in neutron–rich systems, extending in the entire volume, single 1p-1h nature
- GT strength and β-half-life, strong improvement with respect to the RPA

Thanks For Your Attention !!!

Relativistic RPA results

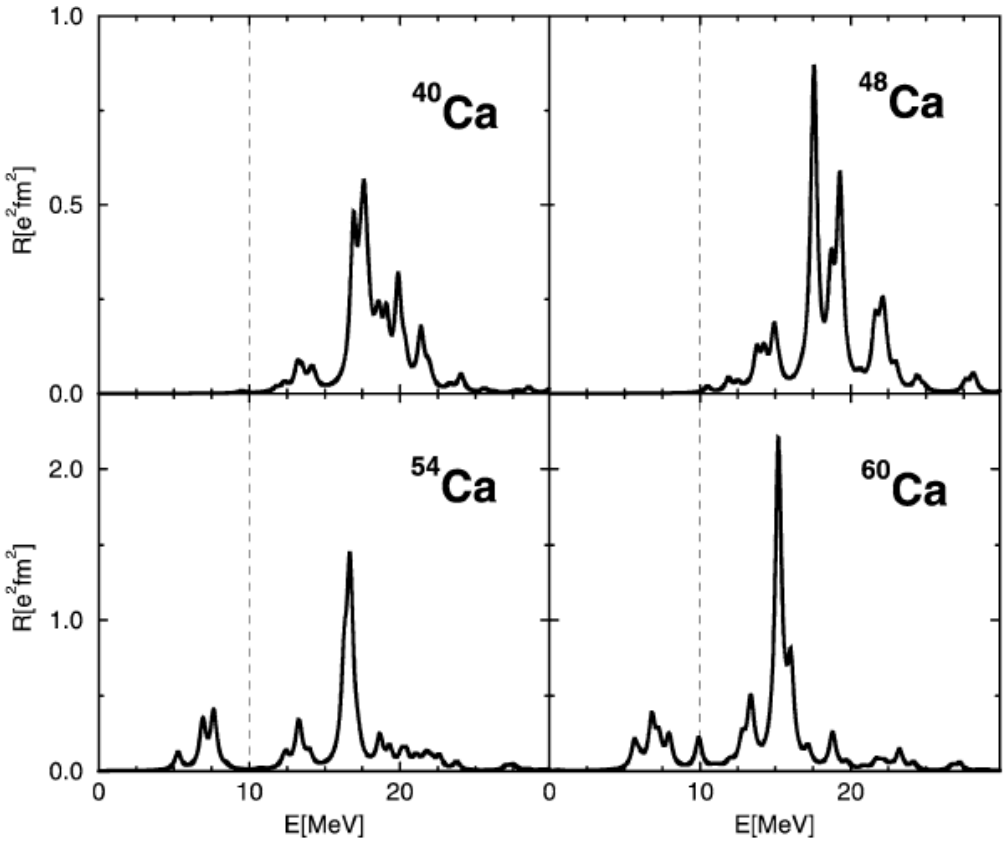

Fig. 5. RRPA isovector dipole strength distributions in Ca isotopes. The thin dashed line tentatively separates the region of giant resonances from the low-energy region below 10 MeV.

From D. Vretenar *et al.*, Nucl. Phys. A 692, 496 (2001)

SSRPA vs Data, GDR case

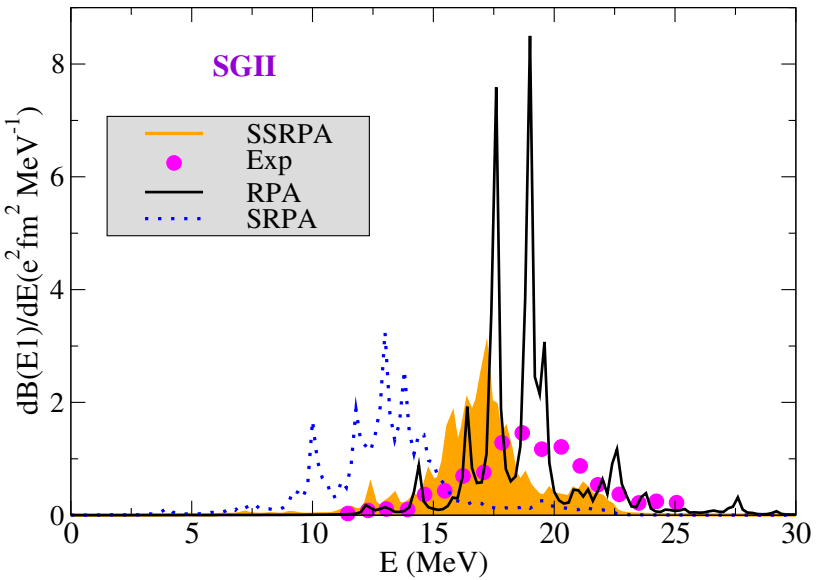

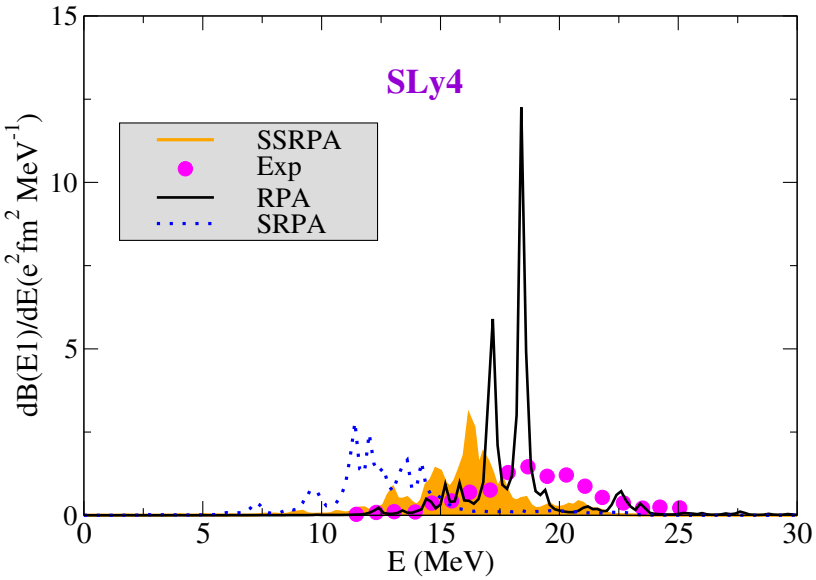

Data From J. Birkhan *et al.*, Phys. Rev. Lett. 118, 252501 (2017);
Theoretical results folded with a Lorentzian having a width of 0.25 MeV
D. G., M. Grasso , O. Vasseur, Physics Letters B 777 (2018) 163–168

SSRPA vs Data, GDR case

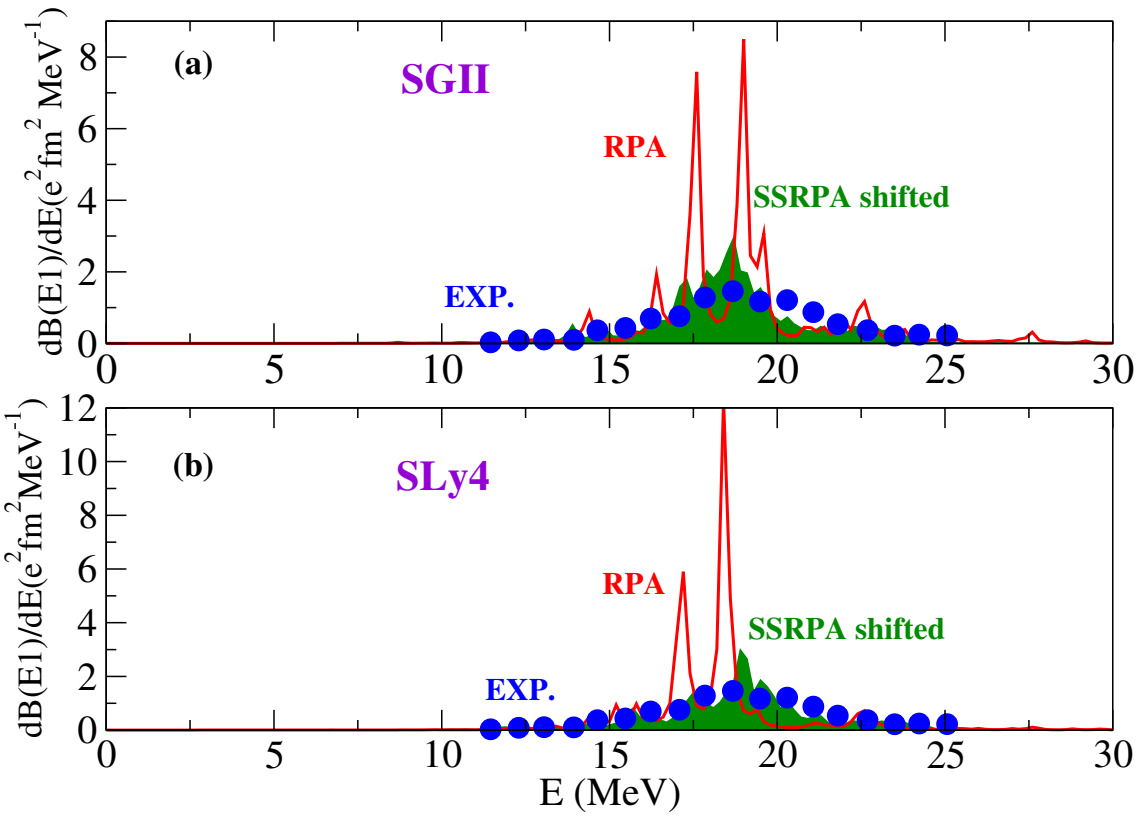

Shift $\sim$ 1 MeV (SGII), $\sim$ 1.5 MeV (SLy4);

SSRPA vs Data, GDR case

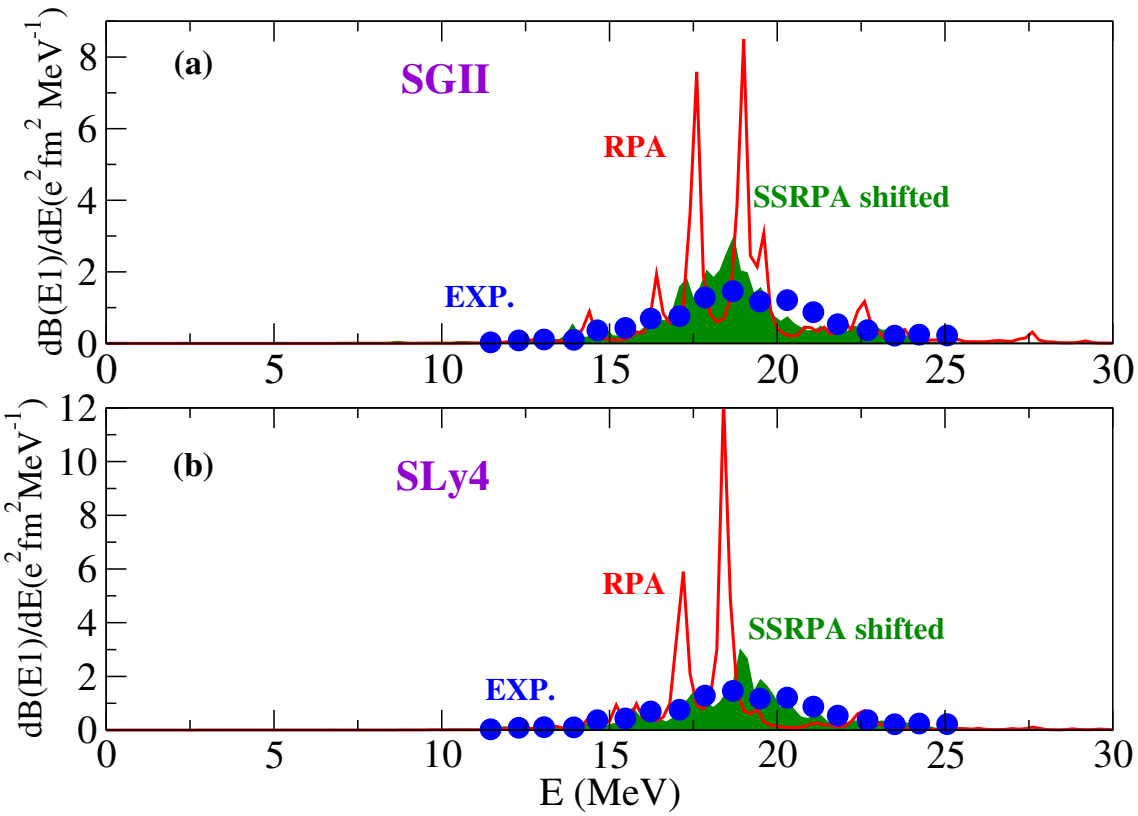

Shift $\sim$ 1 MeV (SGII), $\sim$ 1.5 MeV (SLy4);
Room to improve on that: full subtraction, see DG *et al.*, Phys. Rev. Lett. 125, 212501 (2020)

Dipole Polarizability

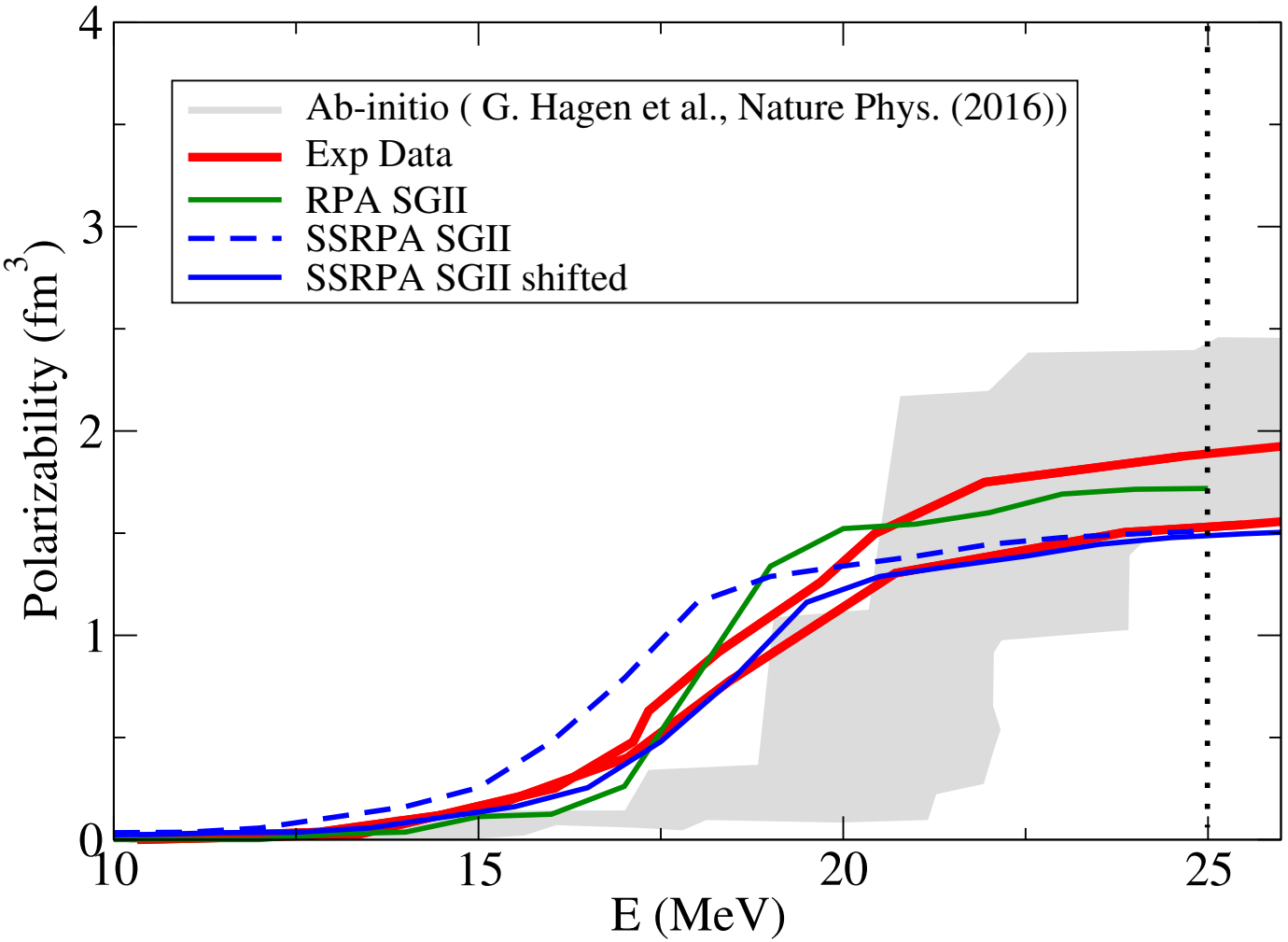

Beyond-mean-field effects on the symmetry energy and its slope

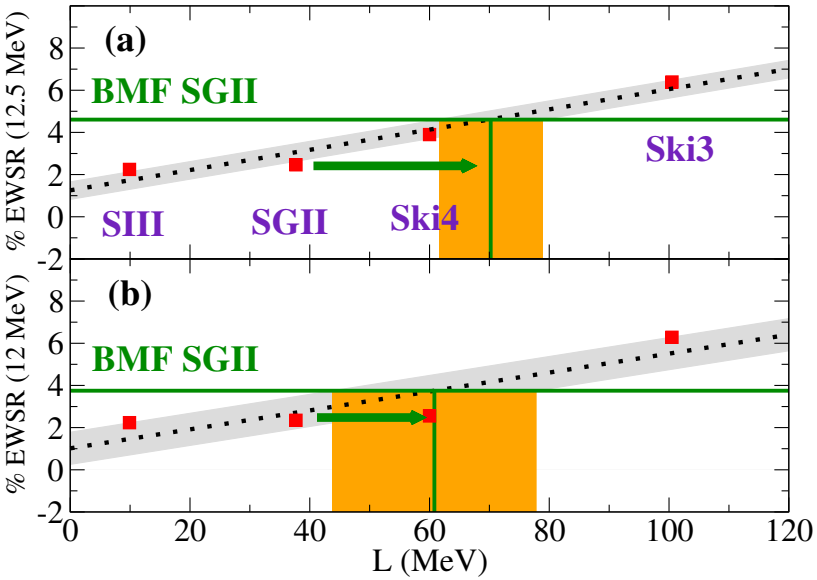

Beyond-mean-field effects on the symmetry energy and its slope

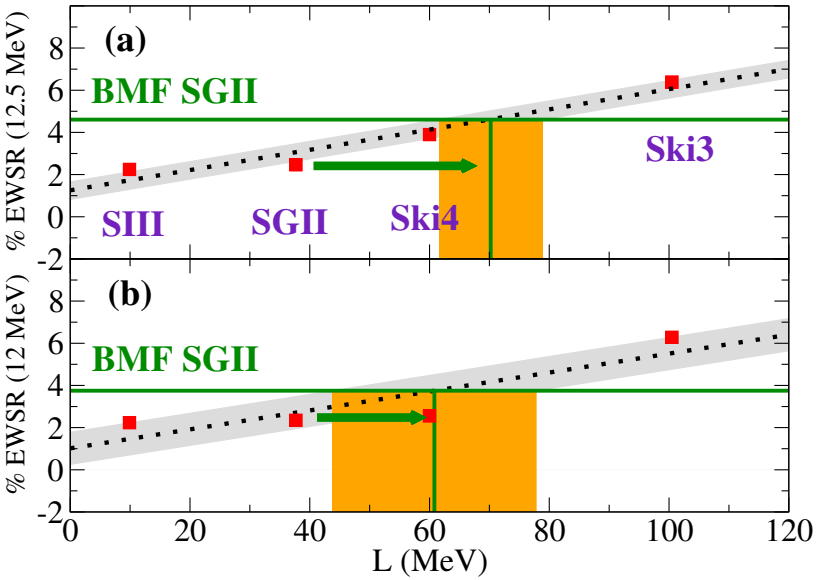

SGII(RPA)= 2.35 %
SGII(SSRPA)=3.75 %

Beyond-mean-field effects on the symmetry energy and its slope

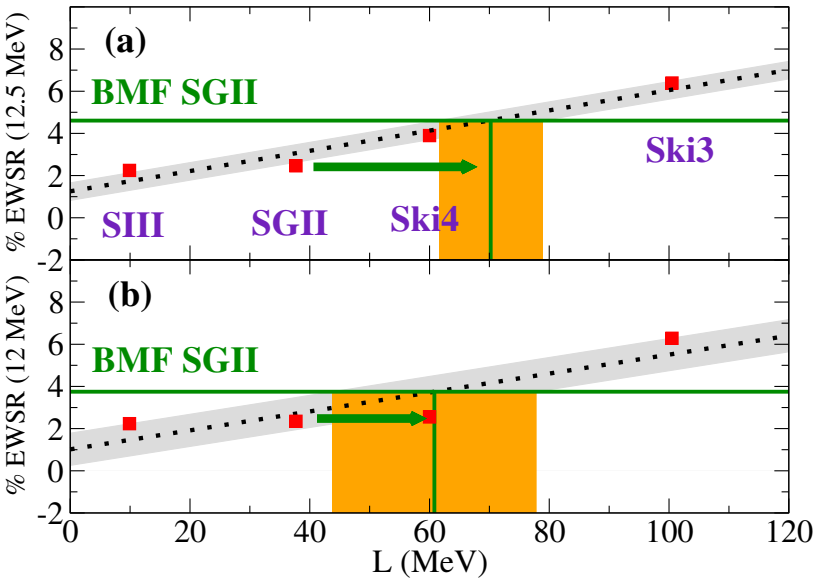

SGII(RPA)= 2.35 %
SGII(SSRPA)=3.75 %

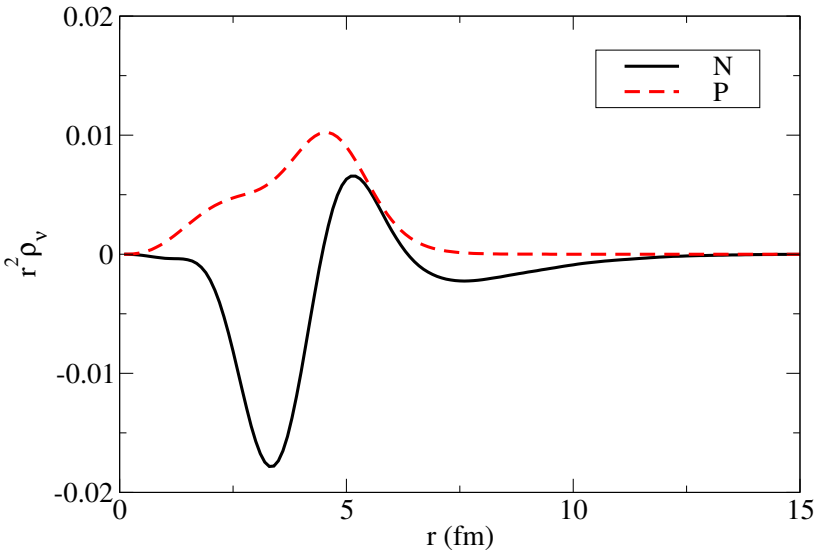

Neutron and proton transition densities for the state located at 12.17 MeV.

Numerical complexity: different approximations schemes

Numerical complexity

- The most demanding task is related to the treatment of the $A_{22'}$ matrix
- The number of 2p-2h configurations can be very large$\simeq 10^7, 10^8$
- We need to calculate the "full" spectrum
- Most demanding tasks:
  a) subtraction procedure, $A_{22'}$ inversion
  b) diagonalization of the SSRPA eigenvalue problem
- Strong simplification if $A_{22'}$ is assumed to be diagonal

Different calculation scheme:

1. SSRPADD: $A_{22'}$ is Diagonal both in a) and b)
2. SSRPADF: $A_{22'}$ is Diagonal both in a) and Full in b)
3. SSRPAFF: $A_{22'}$ is Full both in a) and in b)

GT$^-$ Strength Distribution ^{48}Ca SSRPA results

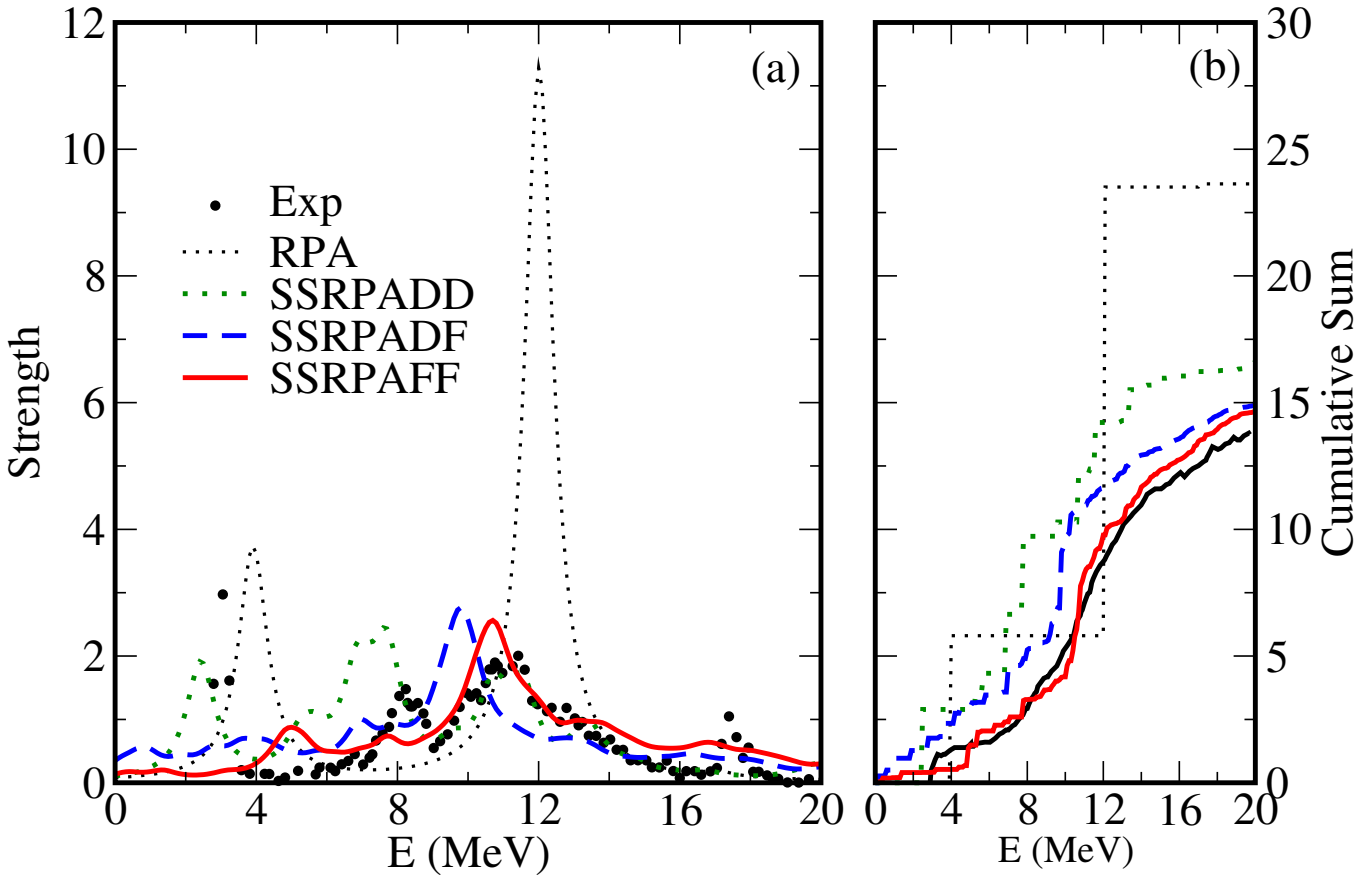

Comparison between SSRPADD, SSRPADF and SSRPAFF results .

From D.Gambacurta and M. Grasso, Phys. Rev. C 105, 014321, (2022)

GT^- Strength Distribution ^{90}Zr SSRPA results

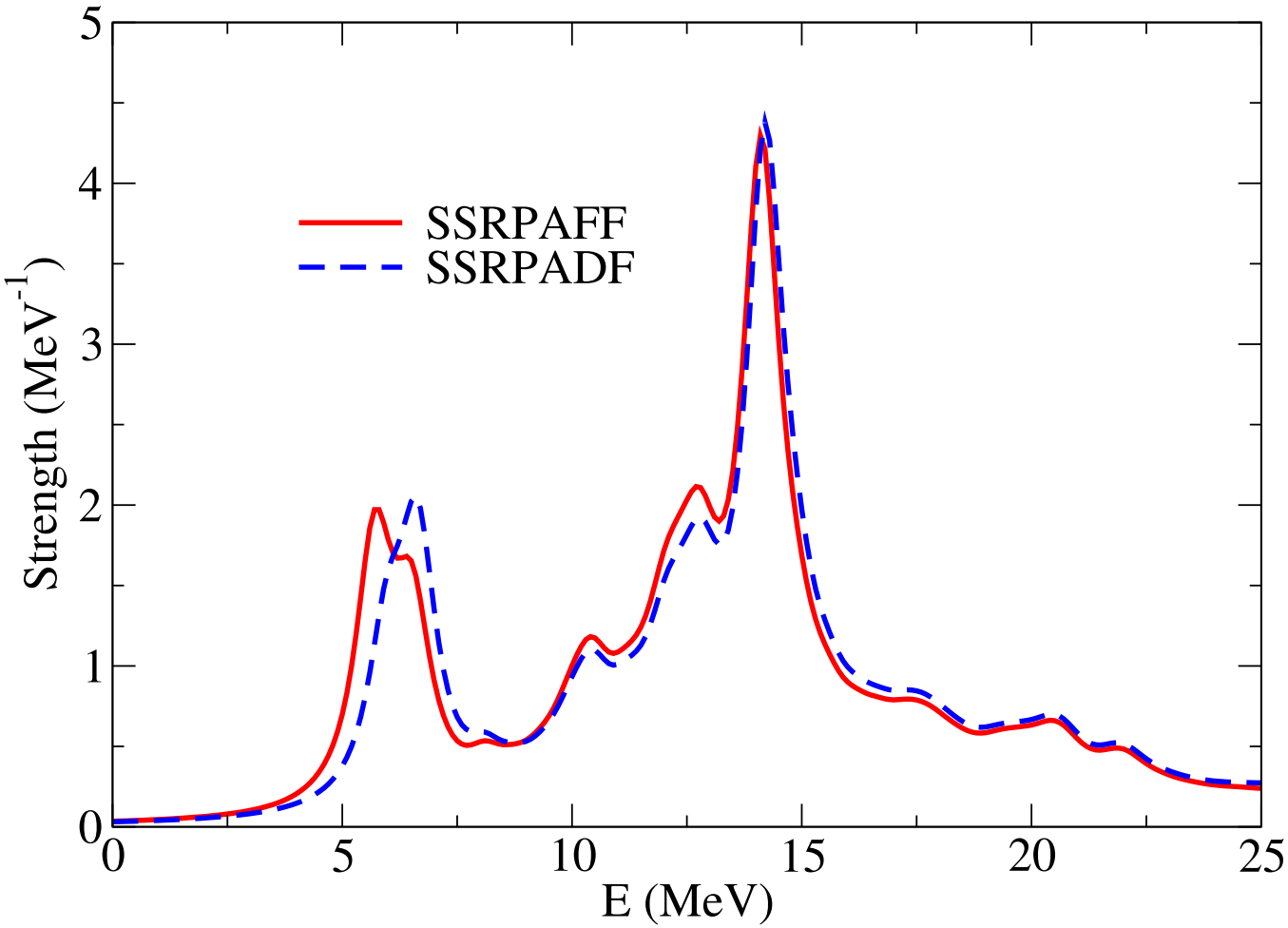

Comparison between SSRPADF and SSRPAFF results .

From D.Gambacurta and M. Grasso, Phys. Rev. C 105, 014321, (2022)

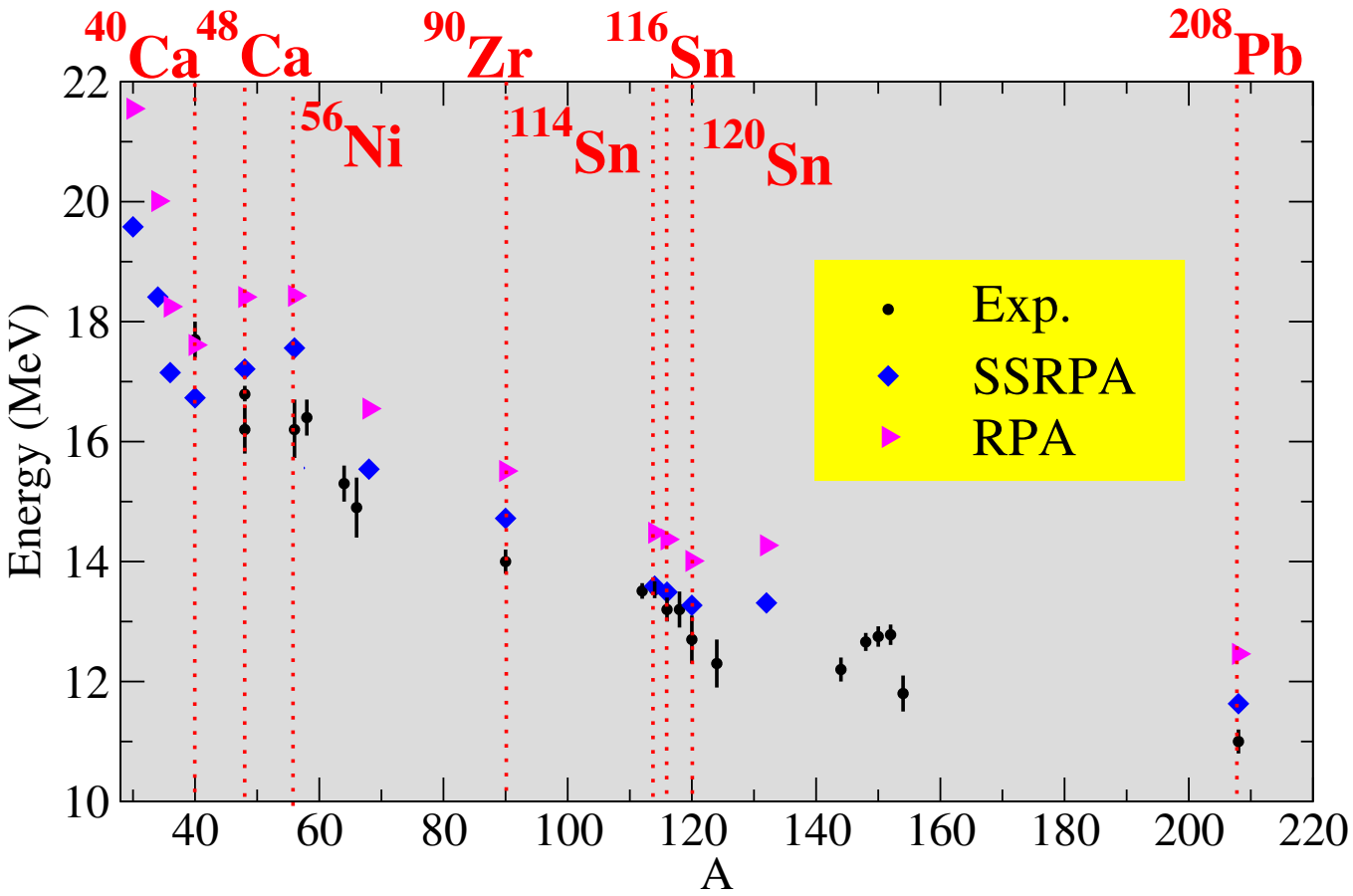

From: O. Vasseur, D. Gambacurta, and M. Grasso,Phys. Rev. C 98, 044313, 2018

GQR systematic study

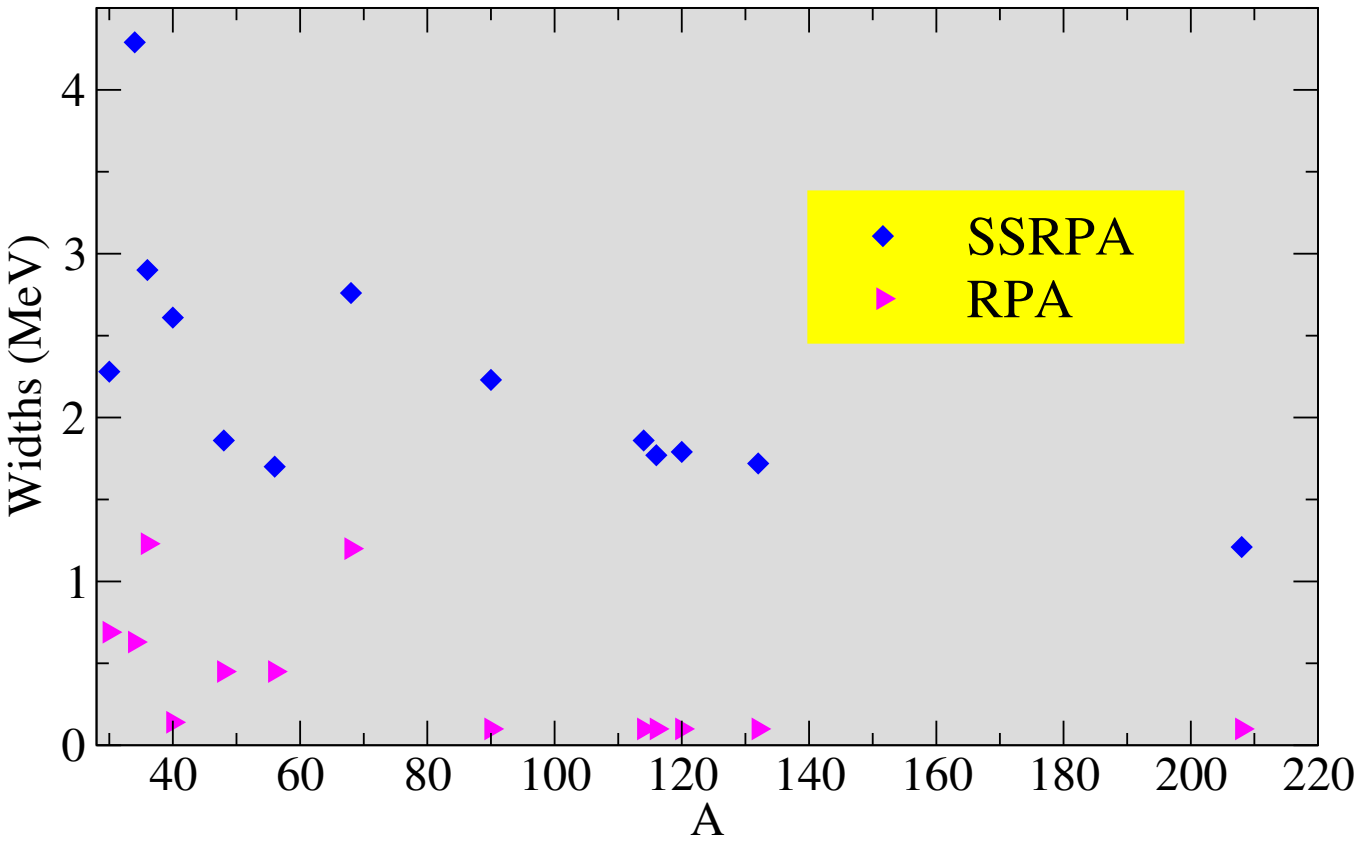

From: O. Vasseur, D. Gambacurta, and M. Grasso,Phys. Rev. C 98, 044313, 2018

GT$^-$ Strength Distribution ^{48}Ca, sum rules in the two channels

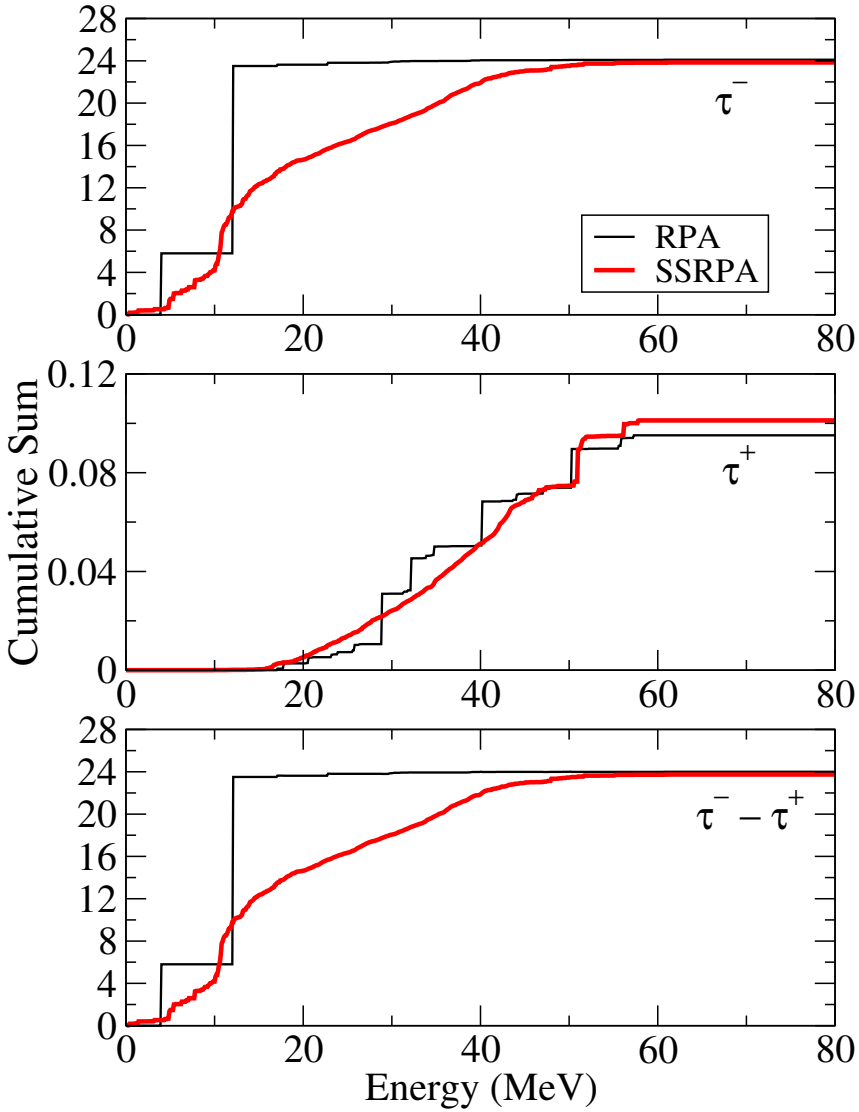

GT^- Strength Distribution ^{48}Ca

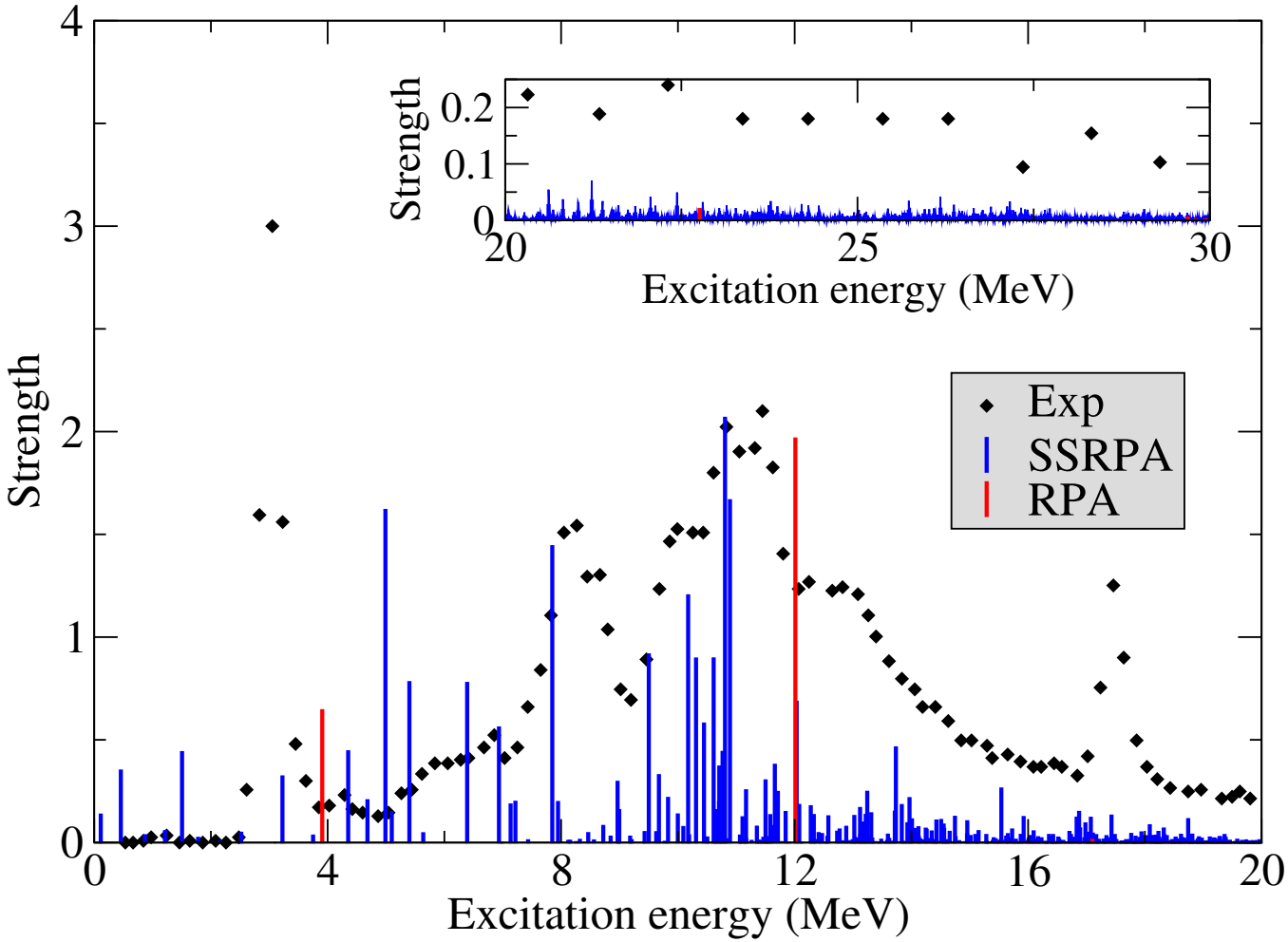

Experimental GT^- in MeV^{-1} and discrete RPA and SSRPA strength distributions (no units) obtained with the Skyrme parameterization SGII, for ^{48}Ca . The RPA strength has been divided by nine and the SSRPA strength by two.

From D.Gambacurta, M. Grasso, J. Engel, Phys. Rev. Lett. 125, 212501 (2020)